APPENDIX A

Marked-Up Version of Claims to Show Changes Made

1. (Amended) A method for inhibiting the proliferation of mammalian cells that express [the] an A_{2B} adenosine receptor comprising administering a therapeutically effective amount of an A_{2B} adenosine receptor antagonist to the [mammal] mammalian cells, whereby the proliferation of cells is inhibited.
2. The method of claim 1 wherein the cells that express the A_{2B} adenosine receptor are vascular endothelial cells.
3. (Amended) The method of claim 2 wherein the vascular endothelial cells that express the A_{2B} adenosine receptor are selected from the group consisting of coronary endothelial cells[,] and endothelial cells from the vascular bed.
4. The method of claim 3 wherein the vascular bed endothelial cells are selected from the group consisting of tumor endothelial cells, retinal endothelial cells, dermal endothelial cells, and brain endothelial cells.
5. (Amended) The method of claim [1] 4 wherein the vascular bed endothelial cells are retinal endothelial cells.
6. The method of claim 1 wherein the A_{2B} adenosine receptor antagonist inhibits the expression of vascular endothelial cell growth factor (VEGF).
7. The method of claim 1 wherein the A_{2B} adenosine receptor antagonist is an A_{2B} adenosine receptor antisense oligonucleotide.
8. The method of claim 1 wherein the A_{2B} adenosine receptor antagonist is an A_{2B}-specific ribozyme.
9. The method of claim 1 wherein the A_{2B} adenosine receptor antagonist is a non-selective adenosine receptor antagonist.
10. The method of claim 1 wherein the A_{2B} adenosine receptor antagonist is a selective A_{2B} adenosine receptor antagonist.
11. (Amended) The method of claim 1 wherein the A_{2B} adenosine receptor antagonist is administered in an amount [raging] ranging from about 1 microgram/kg to about 50 milligrams/kg.
12. (Amended) The method of claim 1 wherein the [adenosine] A_{2B} adenosine receptor antagonist is administered in an amount ranging from about 1 microgram/kg to about 10 milligrams/kg.
13. The method of claim 1 wherein the A_{2B} adenosine receptor antagonist is administered by a method selected from the group consisting of orally, nasally, transdermally, by bolus, intravenously, in eye drops, by inhalation, and by using micropumps.
14. (Amended) The method of claim 1 wherein the A_{2B} adenosine receptor [agonist] antagonist is administered in eye drops.
15. The method of claim 1 wherein the mammal is a human.

The EMBO Journal vol.14 no.21 pp.5224-5229, 1995

A synthetic, chemically modified ribozyme eliminates amelogenin, the major translation product in developing mouse enamel *in vivo*

S.P.Lyngstadaas[1,2], S.Risnes[2], B.S.Sproat[3], P.S.Thrane[4] and H.P.Prydz[1,5]

[1]Biotechnology Centre of Oslo and Laboratory Animal Unit, The National Hospital, University of Oslo, PO Box 1125, Blindern, N-0317 Oslo, [2]Department of Oral Biology, Faculty of Dentistry, University of Oslo, PO Box 1052, Blindern, N-0316 Oslo, [4]Department of Pathology, The Norwegian Radium Hospital, Montebello, N-0310 Oslo, Norway and [3]Ribonetics GmbH, Rudolf-Wissel-Strasse 28, D-37079 Göttingen, Germany

[5]Corresponding author

Ribozymes are small RNA structures capable of cleaving RNA target molecules in a catalytic fashion. Designed ribozymes can be targeted to specific mRNAs, blocking their expression without affecting normal functions of other genes. Because of their specific and catalytic mode of action ribozymes are ideal agents for therapeutic interventions against malfunctioning or foreign gene products. Here we report successful experiments to 'knock out' a major translation product *in vivo* using synthesized, chemically modified ribozymes. The ribozymes, designed to cleave amelogenin mRNA, were injected close to developing mandibular molar teeth in newborn mice, resulting in a prolonged and specific arrest of amelogenin synthesis not caused by general toxicity. No carriers were required to assist cellular uptake. Amelogenins are highly conserved tissue-specific proteins that play a central role in mammalian enamel biomineralization. Ultrastructural analyses of *in vivo* ribozyme-treated teeth demonstrated their failure to develop normally mineralized enamel. These results demonstrate that synthesized ribozymes can be highly effective in achieving both timed and localized 'knock-out' of important gene products *in vivo*, and suggest new possibilities for suppression of gene expression for research and therapeutic purposes.

Keywords: 2'-*O*-allylribonucleotides/amelogenin/biomineralization/dental enamel/synthetic hammerhead ribozymes

Introduction

Interference with gene expression at the level of mRNA holds great promise for therapeutic interventions in cases of malfunctioning gene products and infectious diseases. Wagner (1994) recently summarized the available experience of using oligodeoxynucleotides for this purpose and listed the criteria that should be rigorously applied in the evaluation of such experiments. Designed hammerhead ribozymes represent an alternative technology with even greater potential advantages. Hammerhead ribozymes are small RNA structures capable of cleaving an RNA target molecule in a catalytic fashion in the presence of Mg^{2+} (Pyle, 1993). They bear a resemblance to enzymes, and contain a catalytic motif made up of three base paired stems and a core of highly conserved, non-complementary nucleotides essential for catalysis (Cech and Uhlenbeck, 1994). Their three-dimensional (3-D) structure and mode of action have recently been elucidated (Uhlenbeck, 1987; Pley *et al.*, 1994; Tuschl *et al.*, 1994). Hammerhead ribozyme activity can be targeted to specific mRNAs by choosing the sequences flanking the catalytic motif. The two hammerhead ribozymes used here were designed to block expression of amelogenin, the major translation product during mammalian tooth enamel matrix synthesis, in mice. The enamel is a unique tissue due to its hardness, which reflects a high degree of mineralization. The mineral component is mainly hydroxyapatite (HAp) in the form of closely packed ultramicroscopic crystals, larger than those in other mineralized mammalian tissues (bone, dentin and dental cementum). The crystals are organized by differential orientation into a basic pattern of prisms (rods) and interprism (interrod), which is common to all mammals. Amelogenins are the main product of ameloblasts (Termine *et al.*, 1980), the single layered, columnar epithelial cells lining the crown of the tooth anlage (Figure 1), and are expressed only in this organ (Chen *et al.*, 1994). Amelogenins are supposed to play a crucial role in mammalian enamel biomineralization, possibly by forming supramolecular structures that control the HAp crystal growth during enamel formation (Fincham *et al.*, 1994). The primary structure of amelogenin derived from cow, pig, rat, mouse and human demonstrates a high degree of sequence homology between these species (Brooks *et al.*, 1994).

The murine amelogenin gene (AMEL) is located distally

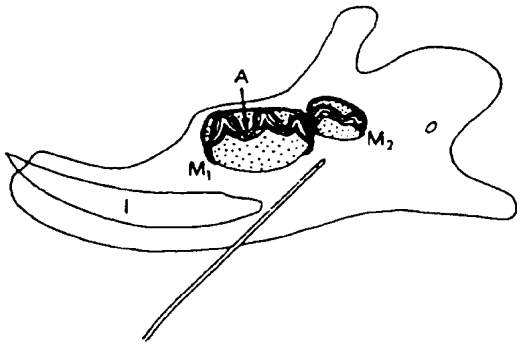

Fig. 1. Lingual view of right mandible of a newborn mouse showing incisor (I) and first (M_1) and second (M_2) molar tooth germs. M_1 where enamel formation has started, and M_2 where enamel formation is about to start (Cohn, 1957; Gaunt, 1964) (M_1 and M_2 depicted as if sectioned). From the tip of the cusps the ameloblasts (A) differentiate in the cervical direction to produce and mature enamel (Sasaki *et al.*, 1990). Needle position during injection is indicated.

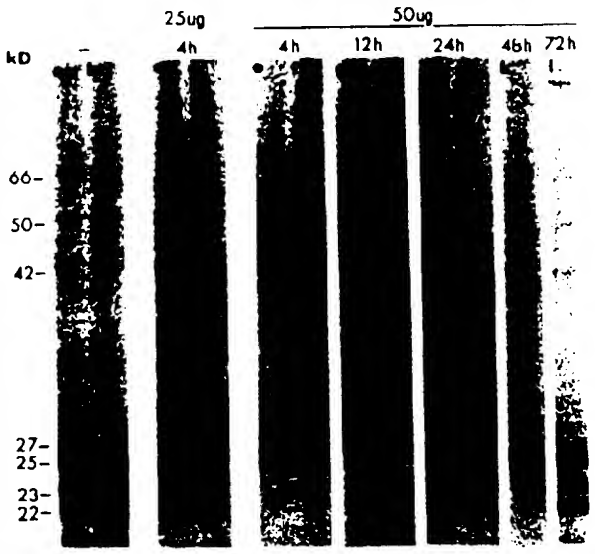

Fig. 2. Autoradiograph of [^{35}S]methionine labelled proteins from normal and ribozyme-treated first molar tooth buds from mandible of newborn mice. Lanes a and b contain proteins from tooth buds of untreated mice. Lanes c and d contain proteins from tooth buds isolated 4 h after injection of 25 µg of the AMEL ribozyme. Lanes e–i contain proteins from tooth buds isolated 4, 12, 24, 48 and 72 h after injection of 50 µg of the AMEL ribozyme. Each lane represents proteins from one half of a first molar tooth bud. The 22, 23, 25 and 27 kDa proteins were identified as amelogenins by protein sequencing. The disappearance of amelogenins indicated a total arrest of their synthesis. All other protein bands appeared unaffected by the ribozyme injection and served as internal controls for the specificity of the AMEL hammerhead ribozyme.

(0.73) on the X chromosome (Lau *et al.*, 1989) and its cDNA has been cloned (Snead *et al.*, 1985). The AMEL gene gives rise to four different polypeptides (Figure 2) caused by differential splicing (Lau *et al.*, 1992). Here we report successful *in vivo* experiments with synthetic hammerhead ribozymes, achieving a specific 'restricted knock out' of the AMEL gene. By local injections (Figure 1) of synthetic ribozyme constructions into newborn mice the major translation product of ameloblasts during the initial stage of enamel formation was eliminated. No carriers were required to assist uptake. The ribozyme effect was monitored both by direct measurement of target protein levels and by loss of biological function. A series of controls demonstrates that the blocking of AMEL expression was specific. Our experiments fulfill the criteria listed by Wagner (1994), and is the first reported study that clearly demonstrates the *in vivo* efficacy of synthesized, chemically modified hammerhead ribozymes.

Results

Effect of the AMEL hammerhead ribozymes

N-terminal amino acid sequences of the 22, 23, 25 and 27 kDa protein bands appearing on SDS–PAGE of molar tooth extracts were revealed by Edman degradation and cyanogen bromide cleavage (Hewick *et al.*, 1981). The protein bands were identified as AMEL proteins when compared with previously reported murine amelogenin protein sequences (Fincham *et al.*, 1991) and were in accordance with the cloned murine AMEL cDNA sequence (Snead *et al.*, 1985). The half-life of amelogenins in molars of newborn mice was determined to be ~210 min in initial pulse–chase experiments where cycloheximide (8 µg/g body weight) and cold methionine (200 µg) were given 100 min after labelled methionine. Amelogenins were isolated and their content of [^{35}S]methionine determined after 100, 200, 300 and 400 min.

When compared with untreated siblings, all ribozyme-injected mice showed a marked decrease in the incorporation of radiolabelled methionine into the amelogenin bands of molar tooth extracts from the injected side after 4 h. Doses of 25 µg ribozyme resulted in a nearly 90% decrease of [^{35}S]methionine in the amelogenin bands. At 50 µg per animal a complete arrest of amelogenin synthesis on the side of injection resulted (Figure 2). This complete arrest of AMEL gene expression lasted ~24 h (Figure 3a). After 3 days amelogenin synthesis was still nearly 50% inhibited. It took 90 h to restore its synthesis to the normal level (100%). After 100 h a brief overexpression (120%) of the AMEL gene was observed. Amelogenin synthesis was back to normal before 120 h and then stabilized at this level.

To see what influence the 3′ terminal phosphorothioate protection of the internucleotide linkages had on ribozyme function and stability, an AMEL hammerhead ribozyme not carrying this modification was applied. Except for a slightly higher and longer lasting efficacy and a slightly more rapid breakdown of the unsulfurized ribozyme, the two AMEL hammerhead ribozymes acted similarly (Figure 3b).

Inhibition of amelogenin synthesis was observed in both the first and the second molar on the side of the injection. In the corresponding contralateral molars a reduction of labelled amelogenins of ~25% was observed at 12 h.

The AMEL hammerhead ribozymes had full activity against all AMEL splice products as none of the four amelogenins appeared in the electrophoresis gels from teeth of ribozyme-treated mice (Figure 2). No other proteins in these gels were affected by the ribozyme injections.

Effect of control injections

Three control oligomers were also designed in order to isolate the ribozyme effects from other oligoribonucleotide effects. One control was an inactive version of the above chemically modified ribozymes in which 'G12' in the conserved hammerhead motif (Haseloff and Gerlach, 1988) was replaced by an 'A', leading to loss of catalytic activity. The second control was a straight antisense oligo(2′-*O*-allylribonucleotide) designed against the same AMEL mRNA region as the ribozymes and applied to distinguish between the ribozyme effect and an ordinary antisense effect. The third control was a randomized oligomer of 18 bases applied for detection of unspecified or toxic actions of the synthetic ribozymes. A fourth control containing only 5 µl sterile saline was included to see whether the injection trauma itself influenced enamel formation.

Injections with the mutated ribozyme gave an immediate inhibition of AMEL expression of >80% (Figure 3c). After 12 h, however, the inhibition was only 40%, and normal levels of amelogenin synthesis were restored within

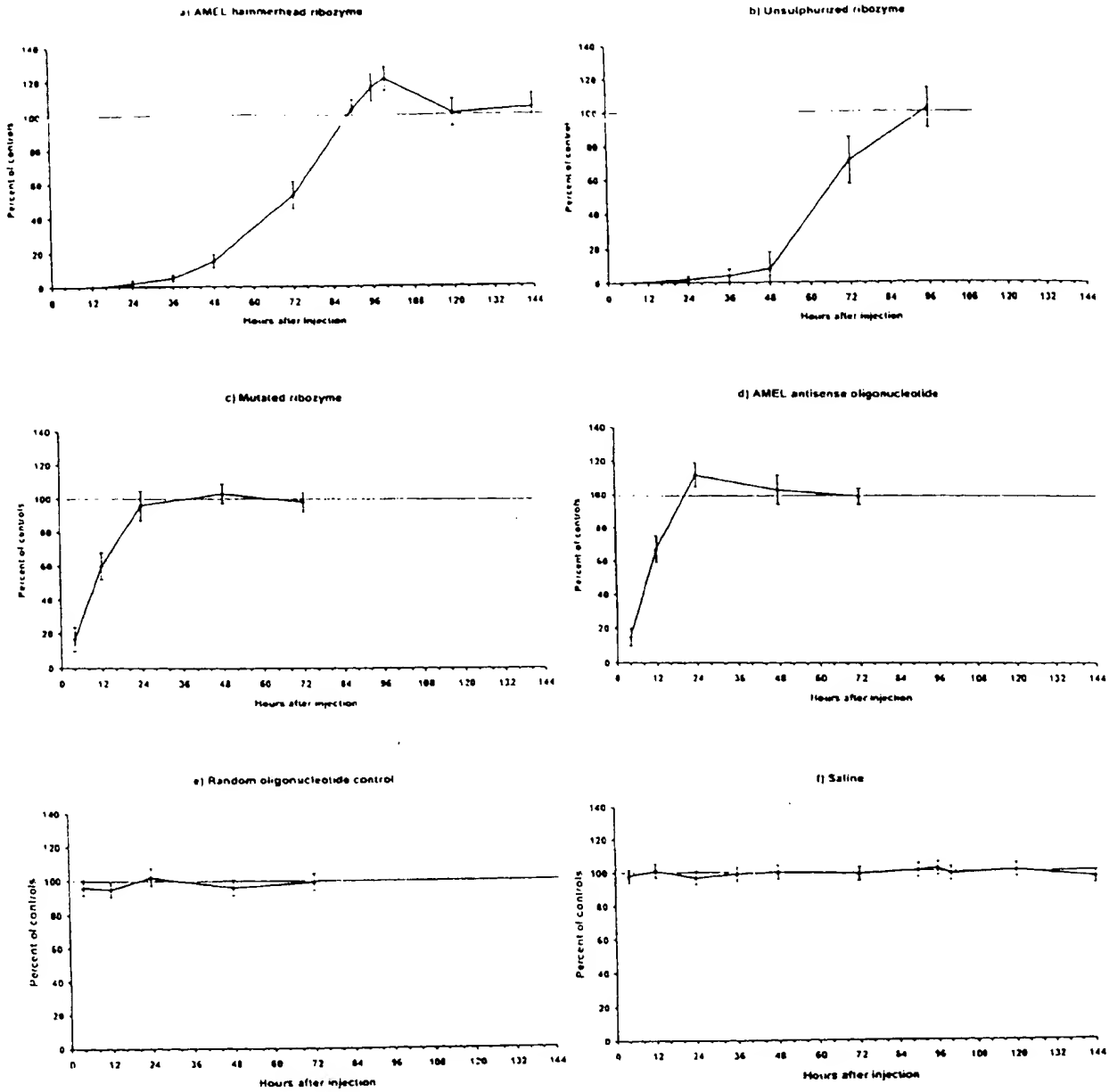

Fig. 3. Effect of injection of AMEL hammerhead ribozymes on [^{35}S]methionine incorporation into amelogenins in newborn mice. Ribozymes and various control oligonucleotides were injected into separate newborn (day 1) mice. Saline injected and untreated litter mates served as controls. The [^{35}S]methionine incorporated into tooth buds was quantitated in a PhosphorImager (Molecular Dynamics). Values are in percent of [^{35}S]methionine incorporated into amelogenins of the corresponding teeth of untreated litter mates, normalized for the size of the available free methionine pool in each tooth bud. These control values are indicated by the 100% line (n = 16 at each time point). (a) AMEL hammerhead ribozyme. Each value is the mean ± SD of four experiments, each with five mice (n = 20). (b) AMEL hammerhead ribozyme without 3' phosphorothioate protected internucleotide linkages. Each value is the mean ± SD of one experiment with five mice (n = 5). (c) Mutated ribozyme (G12→A). Each value is the mean ± SD of two experiments, each with five mice (n = 10). (d) AMEL antisense oligonucleotide (n = 10). (e) Random oligonucleotide controls (n = 8). (f) Saline controls (n = 8).

24 h. In contrast to earlier *in vitro* experiments with antisense oligo(2'-*O*-allylribonucleotide)s (Johansson *et al.*, 1994), the straight antisense oligoribonucleotide injections produced an effect much like that of the mutated ribozyme, initially inhibiting AMEL expression by 80% (Figure 3d), after 12 h inhibition was only 30%, and normal amelogenin synthesis levels were restored before 24 h. Random oligonucleotide injections or saline injections had essentially no influence on the monitored protein synthesis, and the quantity of incorporated [^{35}S]methionine in these animals did not differ significantly from that of their untreated siblings (Figure 3e and f).

Control injections of 5 µl 0.5% Trypan Blue in saline were used to mark the area of diffusion of the injected fluid. The dye could easily be demonstrated in the mandibular molar tooth buds within 30 min after injection.

Fig. 4. SEM micrographs of mouse molar inner enamel abutting on dentin (D). (**a** and **c**) Normal control enamel with structure similar to rat enamel (Risnes, 1979a,b). (**b** and **d**) Corresponding regions of enamel affected by the AMEL hammerhead ribozymes. Prisms (P) of adjacent prism rows are oppositely oriented (unlabelled arrows). The interprism (IP) separates individual prisms. The affected enamel is severely hypomineralized with an accumulation of organic material at the prism periphery–interprism and with no visible HAp crystals within cross-cut prism domains. Magnification bar, 5 μm.

Scanning electron microscopy observations

To look at the effect of the ribozyme on enamel formation, randomly selected mice injected with active ribozyme on day 1 after birth were sacrificed at 5 weeks of age, when their molar teeth were fully developed. Mice injected with the randomized oligonucleotide or saline only and untreated siblings were included as controls. The mandibular molars from these mice were prepared for scanning electron microscopy (SEM) (Risnes, 1985). Molars from ribozyme-treated mice revealed severely disturbed enamel with a pronounced hypomineralization and accumulation of organic material at the prism periphery–interprism, whereas cross-cut prisms appeared as empty holes with no visible HAp crystals present (Figure 4). The general design of the prism pattern and the enamel thickness appeared unaffected. Molars from untreated, saline injected or random oligonucleotide-treated mice showed no such changes. Regions with normal enamel were also observed in teeth from ribozyme-treated animals. Second molars were more severely affected than first molars. No differences were detected in eruption-time or macroscopic tooth morphology between ribozyme-treated, randomized oligonucleotide-treated, saline injected or untreated mice.

Discussion

The AMEL hammerhead ribozyme motif (Haseloff and Gerlach, 1988) was flanked by two AMEL mRNA binding regions (6 and 7 bp, respectively), chosen to optimize the catalytic activity of the ribozyme without losing specificity (Goodchild and Kohli, 1991). Its target was the GUC sequence of the mouse AMEL gene in which the G is at base 86 of the mRNA (Snead *et al.*, 1985). The proposed hammerhead ribozymes were chemically modified (Paolella *et al.*, 1992; Sproat *et al.*, 1994) to contain mostly 2′-*O*-allylribonucleotides and only five ribonucleotides required for catalysis, *viz.* G5, A6, G8, G12 and A15, using the standard numbering system (Hertel *et al.*, 1992), so as to have long term stability *in vivo*. The allylation of U4 is essential to block RNase A attack at this position. In addition, one of the two otherwise identical AMEL hammerhead ribozymes, the mutated ribozyme and the antisense oligoribonucleotide, carried two sulfurized 3′-proximal internucleotide linkages to reduce 3′-exonuclease attack further.

Global 2′-*O*-allylation of oligoribonucleotides confers nuclease resistance, chemical stability, in hybridization high specificity for RNA over DNA and minimal non-specific binding (Iribarren *et al.*, 1990; Lamond and Sproat, 1993), all of which are essential requirements for *in vivo* experiments. Cellular uptake may also be facilitated because of the increased hydrophobicity imparted by 2′-*O*-allylation.

The ribozymes used here totally inhibited expression of the AMEL gene in newborn mice without affecting normal functions of other genes. Apparently, no other proteins were affected by the ribozyme injections (Figure 2), thus constituting a valuable internal control for the specificity of the ribozymes.

The fact that the control dye was detectable in the tooth buds within 30 min, the observed rapid loss of AMEL expression and the fact that amelogenins are produced within ameloblasts only (Chen *et al.*, 1994), provide strong evidence that the modified oligoribonucleotides effectively reach and penetrate these cells, as has been demonstrated for oligodeoxynucleotides when applied to cultured tooth organs (Diekwisch *et al.*, 1993).

The mutated ribozyme and the antisense oligoribonucleotide showed similar effects during the first 12 h. This suggests that the amelogenin-specific hybridizing arms of the mutated ribozyme make it act like an ordinary antisense oligoribonucleotide inhibiting amelogenin synthesis for a short period, possibly by temporary blockage of ribosome progression along mRNA and that the hammerhead motif itself does not affect the specific binding of its flanking regions to amelogenin mRNAs.

Injections containing the randomized oligonucleotide had essentially no influence on AMEL expression (Figure 3d), nor did they produce any structural defects in the mature enamel. This indicates that the observed ribozyme effect was not due to a non-specific or toxic influence of oligonucleotides on AMEL expression. Neither did mice injected with saline show any significant difference from their untreated siblings, indicating that the injections themselves did not affect protein synthesis or function in developing enamel.

The slightly increased efficacy of the ribozyme not protected by 3′ phosphorothioate internucleotide linkages might reflect an enhanced cellular uptake of this oligomer. The apparent slightly more rapid cessation of its effect may be due to a more rapid breakdown caused by an increased sensitivity to 3′-exonuclease attack on this ribozyme.

The difference in occurrence of enamel defects among first and second molars reflects the different developmental stages of these teeth at the time of ribozyme injection. The fact that the second molar was more severely affected than the first molar indicates that amelogenin plays a key role at a very early stage in enamel development and may be less important at later stages. Areas with normal enamel formation within each affected tooth represent early (occlusal) and late (cervical) enamel matrix synthesis unaffected by the time-limited ribozyme effect applied here.

Designed hammerhead ribozymes are promising agents for blocking specific gene expression. Chemical modifications enhance their stability, potency and ability to enter cells. As the 3-D structures of the hammerhead motifs are revealed, even more effective ribozymes can be developed. The tooth model lends itself nicely to the study of ribozyme function *in vivo* since the biological consequences of the ribozyme effect are permanently displayed in the mature enamel. We report the first demonstration of *in vivo* efficacy of synthesized, chemically modified ribozymes. Only a few cases of specific gene inhibition caused by antisense oligodeoxynucleotides have been rigorously demonstrated in cultured cells before (Wagner, 1994). Our experiments clearly illustrate the advantages of combining the catalytic activity of a hammerhead motif with the specificity of antisense oligomers in a chemically modified oligoribonucleotide to obtain both enhanced and prolonged specific blocking of gene expression *in vivo*. The strategy used in this model could be highly effective in achieving both timed and localized 'knock-outs' of important gene products *in vivo*, and suggests new possibilities for suppression of gene expression for research and therapeutic purposes.

Materials and methods

Oligoribonucleotide synthesis

The AMEL hammerhead ribozyme (5′-UGUUGACUgaUgAGGCCGUUAGGCCgAAaCAGC*PS*A*PS*C), the unsulfurized ribozyme (5′-UGUUGACUgaUgAGGCCGUUAGGC CgAAaCAGCAC), the mutated ribozyme (5′-UGUUGACUgaUgAGGCCGUUAGGCCaAAaCAGC*PS*A*PS*C), the straight antisense oligo(2′-*O*-allylribonucleotide)(5′-UGUUGAGACAGC*PS*A*PS*C) and the 18mer randomized oligonucleotide (scrambled, unmodified) were synthesized on solid-phase using phosphoramidite chemistry (capital letters are 2′-*O*-allylribonucleotides and lower case letters are ribonucleotides, phosphorothioate protected internucleotide linkages are denoted *PS*, underlined sequences are complementary to the AMEL target sequence). The ribonucleotides carried standard 2′-*O*-*tert*-butyldimethylsilyl protection, which was subsequently removed by treatment of the partially deprotected oligomer with neat triethylamine trihydrofluoride (Gasparutto *et al.*, 1992). The oligonucleotides were purified by HPLC before injection.

Experimental design

Oligoribonucleotides were dissolved in sterile saline to a final concentration of 10 μg/μl each, and 50 μg of each delivered by submandibular injection into five newborn BALB/C (albino) mice without addition of liposomes or other vehicles to enhance cellular uptake. On the first day after birth each animal received an injection of ribozyme or control oligonucleotides on the lingual side of the right mandibular molar area. Other controls received 5 μl saline. A reference group of untreated

siblings of the experimental animals was included to monitor the normal AMEL expression in these mice.

Injections of 5 µl 0.5% Trypan Blue in saline were used to mark the area of diffusion. All injections were carried out using a Hamilton syringe with a 0.3 mm needle at the rate of ~1 µl/s. At 0, 8, 20, 32, 44, 68, 86, 92, 96, 116 or 140 h after the mandibular injections experimental animals and a reference group received a 4 h pulse of 20 µCi [^{35}S]methionine (Amersham) given i.p. The mice were then sacrificed and their mandibular molar tooth buds were dissected out. Each tooth bud was rinsed in sterile saline and boiled in 50 µl 2× SDS–PAGE sample buffer (0.4 g SDS, 1.0 g 2-mercaptoethanol, 0.02 g bromophenol blue and 4.4 g glycerol in 10 ml 0.125 M Tris–HCl, pH 6.8) for 5 min. Half of each sample was then submitted to electrophoresis on 12% SDS–polyacrylamide gels at 80 mA overnight. The gels were dried and placed in a PhosphorImager (Molecular Dynamics) to detect radioactive methionine incorporated into the proteins present. Subsequently, the gels were submitted to ordinary autoradiography for 30 days as a visual control. Proteins in the other half of each sample were precipitated with 0.6 N perchloric acid (PCA) and the supernatant was cleared by centrifugation. The free radiolabelled methionine in the supernatant was measured in a Packard Tricarb Scintillation counter and used to normalize the values from the PhosphorImager so that individual differences in the availability of radiolabelled methionine were adjusted for.

Scanning electron microscopy

Randomly selected mice injected once with the AMEL hammerhead ribozyme on day 1 after birth were sacrificed at 5 weeks of age, when their molar teeth were fully developed and erupted. Mice injected with the randomized 18mer oligonucleotide and with saline only, and untreated siblings were included as controls. The mandibular molars from these mice were dissected out, taking care not to damage enamel structures, and prepared for scanning electron microscopy (SEM) by sectioning and grinding (Risnes, 1985), etching three times for 10 s in 0.1% nitric acid and sputter-coating with gold–palladium. A Phillips 515 SEM was operated at 15 kV.

Protein sequencing

Amelogenin protein bands separated by SDS–PAGE were transferred onto a poly(vinylidene difluoride) membrane by the semi-dry 'sandwich' electroblotting technique (Matsudaira, 1987). The membrane was stained with Coomassie Blue and the four amelogenin bands cut out, separated and submitted to Edman degradation and *in situ* cyanogen bromide cleavage (Hewick *et al.*, 1981).

N-terminal amino acid sequences were analyzed with an Applied Biosystems 477A instrument coupled to a 120A analyzer. After a sufficient number of Edman degradation cycles, the remaining filter-bound polypeptides were cleaved *in situ* with CNBr. The filters with the adhering polypeptides were placed in Eppendorf tubes, 30 µl CNBr solution (0.2 g/ml 70% formic acid) was applied to the filters, and an extra 30 µl was placed in the bottom of each tube, below the filters, to keep them moist. Nitrogen gas was introduced, after which the tubes were sealed and incubated for 24 h in the dark. Following this treatment, the filters were dried under vacuum and reapplied to the sequencer.

Acknowledgements

This work was supported by grants to H.Prydz from the Research Council of Norway and the Norwegian Cancer Society. We are grateful to Professor K.Sletten for sequencing the amelogenins, to D.Sorensen and his staff for the use of the animal facilities and to Dr A.Hogseth for access to the PhosphorImager.

References

Brooks,S.J., Bonass,W.A., Kirkham,C. and Robinson,C. (1994) The human C-terminal sequence is completely homologous to the C-terminal sequence of amelogenin in all species so far studied. *J. Dent. Res.*, **73**, 716.

Cech,T.R. and Uhlenbeck,O.C. (1994) Hammerhead nailed down. *Nature*, **372**, 39–40.

Chen,E. *et al.* (1994) Regulation of amelogenin gene expression during tooth development. *Dev. Dyn.*, **199**, 189–198.

Cohn,S.A. (1957) Development of the molar teeth of the albino mouse. *Am. J. Anat.*, **101**, 295–320.

Diekwisch,T., David,S., Bringas,P.,Jr, Santos,V. and Slavkin,H.C. (1993) Antisense inhibition of AMEL translation demonstrates supramolecular controls for enamel HAP crystal growth during embryonic molar development. *Development*, **117**, 471–482.

Fincham,A.G., Hu,Y., Lau,E.C., Slavkin,H.C. and Snead,M.L. (1991) Amelogenin post-secretory processing during biomineralization in the postnatal mouse molar tooth. *Arch. Oral Biol.*, **36**, 305–317.

Fincham,A.G. *et al.* (1994) Self-assembly of a recombinant amelogenin protein generates supramolecular structures. *J. Struct. Biol.*, **112**, 103–109.

Gasparutto,D. *et al.* (1992) Chemical synthesis of a biologically active natural tRNA with its minor bases. *Nucleic Acids Res.*, **20**, 5159–5166.

Gaunt,W.A. (1964) The development of the teeth and jaws of the albino mouse. *Acta Anat.*, **57**, 115–151.

Goodchild,J. and Kohli,V. (1991) Ribozymes that cleave an RNA sequence from human immunodeficiency virus: The effect of flanking sequence on rate. *Arch. Biochem. Biophys.*, **284**, 386–391.

Haseloff,J. and Gerlach,W.L. (1988) Simple RNA enzymes with new and highly specific endoribonuclease activities. *Nature*, **334**, 585–591.

Hertel,K.J. *et al.* (1992) Numbering system for the hammerhead. *Nucleic Acids Res.*, **20**, 3252.

Hewick,R.M., Hunkapiller,M.W., Hood,L.E. and Dreyer,W.J. (1981) A gas-liquid solid phase peptide and protein sequenator. *J. Biol. Chem.*, **256**, 7990–7997.

Iribarren,A.M. *et al.* (1990) 2′-*O*-alkyl oligoribonucleotides as antisense probes. *Proc. Natl Acad. Sci. USA*, **87**, 7747–7751.

Johansson,H.E., Belsham,G.J., Sproat,B.S. and Hentze,M.W. (1994) Target-specific arrest of mRNA translation by antisense 2′-O-alkyloligoribonucleotides. *Nucleic Acids Res.*, **22**, 4591–4598.

Lamond,A.I. and Sproat,B.S. (1993) Antisense oligonucleotides made of 2′-*O*-alkylRNA: their properties and applications in RNA biochemistry. *FEBS Lett.*, **325**, 123–127.

Lau,E.C., Mohandas,T.K., Saphiro,L.J., Slavkin,H.C. and Snead,M.L. (1989) Human and mouse amelogenin gene loci are on the sex chromosomes. *Genomics*, **4**, 162–168.

Lau,E.C. *et al.* (1992) Alternative splicing of the mouse amelogenin primary RNA transcript contributes to amelogenin heterogeneity. *Biochem. Biophys. Res. Commun.*, **188**, 1253–260.

Matsudaira,P. (1987) Sequence from picomole quantities of proteins electroblotted onto poly(vinylidene difluoride) membranes. *J. Biol. Chem.*, **262**, 10035–10038.

Paolella,G., Sproat,B.S. and Lamond,A.I. (1992) Nuclease resistant ribozymes with high catalytic activity. *EMBO J.*, **11**, 1913–1919.

Pley,H.W., Flaherty,K.M. and McKay,D.B. (1994) Three-dimensional structure of a hammerhead ribozyme. *Nature*, **372**, 68–74.

Pyle,A.M. (1993) Ribozymes: A distinct class of metalloenzymes. *Science*, **261**, 709–714.

Risnes,S. (1979a) A scanning electron microscope study of aberrations in the prism pattern of rat incisor inner enamel. *Am. J. Anat.*, **154**, 419–436.

Risnes,S. (1979b) The prism pattern of rat molar enamel: a scanning electron microscope study. *Am. J. Anat.*, **155**, 245–257.

Risnes,S. (1985) Multiangular viewing of dental enamel in the SEM: an apparatus for controlled mechanical specimen preparation. *Scand. J. Dent. Res.*, **93**, 135–138.

Sasaki,T., Goldberg,M., Takuma,S. and Garant,P.R. (1990) Cell biology of tooth enamel formation. Functional electron microscopic monographs. *Monogr. Oral Sci.*, **14**, 1–199.

Snead,M.L. *et al.* (1985) DNA sequence for cloned cDNA for murine amelogenin reveal the amino acid sequence for enamel-specific protein. *Biochem. Biophys. Res. Commun.*, **129**, 812–818.

Sproat,B.S., Lamond,A.I. and Paolella,G. (1994) *US Patent 5*, **334**, 711.

Termine,J.D., Belcourt,A.B., Christner,P.J., Conn,K.M. and Nylen,M.U. (1980) Properties of dissociatively extracted fetal tooth matrix proteins. I. Principal molecular species in developing bovine enamel. *J. Biol. Chem.*, **225**, 9760–9768.

Tuschl,T., Gohlke,C., Jovin,T.M., Westhof,E. and Eckstein,F. (1994) A three-dimensional model for the hammerhead ribozyme based on fluorescence measurements. *Science*, **266**, 785–789.

Uhlenbeck,O.C. (1987) A small catalytic oligoribonucleotide. *Nature*, **328**, 596–600.

Wagner,R.W. (1994) Gene inhibition using antisense oligodeoxynucleotides. *Nature*, **372**, 333–335.

Received on June 28, 1995; revised on August 14, 1995

Proc. Natl. Acad. Sci. USA
Vol. 91, pp. 2051–2055, March 1994
Biochemistry

Ribozyme-mediated attenuation of pancreatic β-cell glucokinase expression in transgenic mice results in impaired glucose-induced insulin secretion

(antisense RNA/β-cell lines/diabetes/glucose phosphorylation/glucose sensing)

SHIMON EFRAT*†, MARGARITA LEISER‡, Y.-JIAN WU§, DAVID FUSCO-DEMANE*, OBAIDULLAH A. EMRAN*, MANJU SURANA‡, THOMAS L. JETTON¶, MARK A. MAGNUSON¶, GORDON WEIR§, AND NORMAN FLEISCHER‡

Departments of *Molecular Pharmacology and ‡Medicine, Albert Einstein College of Medicine, Bronx, NY 10461; §Joslin Diabetes Center, Boston, MA 02215; and ¶Department of Molecular Physiology and Biophysics, Vanderbilt University School of Medicine, Nashville, TN 37232

Communicated by Frank Lilly, November 22, 1993

ABSTRACT **Phosphorylation of glucose to glucose 6-phosphate by glucokinase (GK; EC 2.7.1.2) serves as a glucose-sensing mechanism for regulating insulin secretion in β cells. Recent findings of heterozygous GK gene mutations in patients with maturity-onset diabetes of the young (MODY), a form of type II (non-insulin-dependent) diabetes characterized by autosomal dominant inheritance, have raised the possibility that a decrease in β-cell GK activity may impair the insulin secretory response of these cells to glucose. To generate an animal model for MODY we have expressed in transgenic mice a GK antisense RNA with a ribozyme element under control of the insulin promoter. Mice in two independent lineages had about 30% of the normal islet GK activity. Insulin release in response to glucose from *in situ*-perfused pancreas was impaired; however, the plasma glucose and insulin levels of the mice remained normal. These mice are likely to be predisposed to type II diabetes and may manifest increased susceptibility to genetic and environmental diabetogenic factors. They provide an animal model for studying the interaction of such factors with the reduced islet GK activity.**

The mechanisms by which pancreatic β cells sense and respond to physiological changes in blood glucose have been the subject of extensive investigation. Glucose-induced insulin secretion requires the metabolism of glucose in β cells (1). The phosphorylation of glucose to glucose 6-phosphate, which determines the rate of glycolysis, has been proposed to constitute a key glucose-sensing mechanism for regulating insulin secretion (2). β cells and hepatocytes express a high-K_m member of the hexokinase family, glucokinase (GK; EC 2.7.1.2), which is responsible for the majority of glucose phosphorylation activity in β cells (2). While in the liver transcription of the GK gene is induced by insulin (3, 4), GK expression in β cells is primarily regulated by glucose at the translational and post-translational levels (3, 5).

Recent DNA polymorphism studies have established a linkage between the GK locus and diabetes in patients with a non-insulin-dependent diabetes mellitus form termed maturity-onset diabetes of the young (MODY) (6, 7). This disease is characterized by an early age of onset and an autosomal dominant inheritance. Sequencing of the GK gene from MODY patients has detected a number of nonsense and missense mutations which are associated with regions of the enzyme molecule involved in glucose and ATP binding (6, 7). The molecular mechanism which makes these mutations dominant remains unknown. The inheritance pattern of the disease suggests that the patients' β cells contain normal enzyme molecules encoded by the wild-type allele. The mutant proteins manifest drastically reduced activities (8, 9). Since GK expression in β cells is not transcriptionally regulated, the wild-type allele cannot compensate for this reduction. The decreased GK activity may be sufficient to shift the threshold for glucose sensing, thereby resulting in impaired insulin secretion at physiological glucose levels. However, it remains unclear whether abnormal glucose uptake by the liver contributes to the disease.

Understanding of the human disease can benefit from an animal model, which will allow detailed biochemical and physiological studies. We sought to generate a mouse model for MODY by specifically reducing GK activity in β cells, without affecting its function in the liver. To this end a GK ribozyme was expressed in β cells in transgenic mice. Ribozymes are RNA molecules that possess catalytic RNA-cleavage activity (10, 11). By flanking the ribozyme catalytic element with two gene-specific fragments in antisense orientation the ribozyme activity can be targeted against a unique RNA sequence, thus reducing target mRNA levels and activity. The transgenic mice expressing the GK ribozyme manifest only a third of the normal islet GK activity. Insulin secretion in response to glucose is impaired; however, the mice remain euglycemic. These findings suggest that GK deficiency in the liver, in addition to that in the islets, may play a role in the induction of diabetes in MODY patients. These mice provide an animal model for studying the interaction of genetic and environmental diabetogenic factors with the reduced islet GK activity.

MATERIALS AND METHODS

Plasmid Constructs. Two oligonucleotides were synthesized containing two 12-base fragments derived from mouse GK gene exon 3 sequence (12) that flank a hammerhead ribozyme catalytic element (10, 11). Annealing of the sense oligonucleotide 5'-GATCCTCTCCCACTTTCTGATGAG-TCCGTGAGGACGAAACCAGCATCACCGGTAC-3' and the antisense oligonucleotide 5'-CGGTGATGCTGGTT-TCGTCCTCACGGACTCATCAGAAAGTGGGAGAG-3' created a fragment (GKRZ) with *Bam*HI and *Kpn* I protruding ends, which was ligated downstream of a hybrid intron element (13) and upstream of the simian virus 40 late polyadenylylation site in pMLSIS.CAT (13). The combined 675-bp fragment was inserted into the *Xba* I and *Sal* I sites of pRIP-Tag (14) downstream of the rat insulin II gene promoter to form pRIP-GKRZ. A DNA fragment containing the neomycin-resistance gene under control of the *pgk* promoter (15)

The publication costs of this article were defrayed in part by page charge payment. This article must therefore be hereby marked "*advertisement*" in accordance with 18 U.S.C. §1734 solely to indicate this fact.

Abbreviations: GK, glucokinase; MODY, maturity-onset diabetes of the young; U, unit(s).

†To whom reprint requests should be addressed.

was inserted into the *Sal* I site of pRIP-GKRZ to form pRIP-GKRZ/neo.

Generation of Transgenic Mice. Linearized pRIP-GKRZ DNA was microinjected into C3HeB/FeJ mouse embryos, and transgenic mice were generated and bred according to established procedures (16).

RNA Analysis. Five million βTC6 cells (17) were electroporated with 30 μg of pRIP-GKRZ/neo DNA in 1 ml of Dulbecco's modified Eagle's medium (DMEM) at 800 μF and 250 V. RNA was extracted from G418-resistant and untransfected cells by using RNA Stat-60 (Tel-Test, Friendswood, TX). Five micrograms of RNA was reverse-transcribed, and 1% of the reaction volume was used in 35 cycles of PCR amplification with sense (5'-CTCTAGAATTCGCTGTCTGCGAGG-3') and antisense (5'-CACTGCATTCTAGTTGTGGTTTGTCC-3') oligonucleotides flanking the intron. The amplified fragments were fractionated on a 1.25% agarose gel, visualized with ethidium bromide, and photographed under UV light. Poly(A)$^+$ mRNA was selected with the Poly(A) Quik kit (Stratagene). Ten micrograms of mRNA was fractionated on a 1% agarose/0.22 M formaldehyde gel, blotted onto nitrocellulose filter, hybridized with a [^{32}P]dCTP-labeled rat GK cDNA probe, and autoradiographed on an x-ray film. The blot was stripped and rehybridized with an α-tubulin probe to normalize for mRNA loading. The autoradiographs were scanned with an LKB Ultroscan XL densitometer.

Immunoblotting. Proteins were extracted from G418-resistant and untransfected cells as described (18). Twenty micrograms of protein was fractionated on a 12% polyacrylamide/SDS gel, electroblotted onto an Immobilon-P filter (Millipore), and probed as described (19) with a sheep anti-GK serum (19). The bound antibody was visualized with a horseradish peroxidase-conjugated second antibody and a chemiluminescent substrate (ECL, Amersham) by exposure to an x-ray film and quantitated by densitometry. Protein

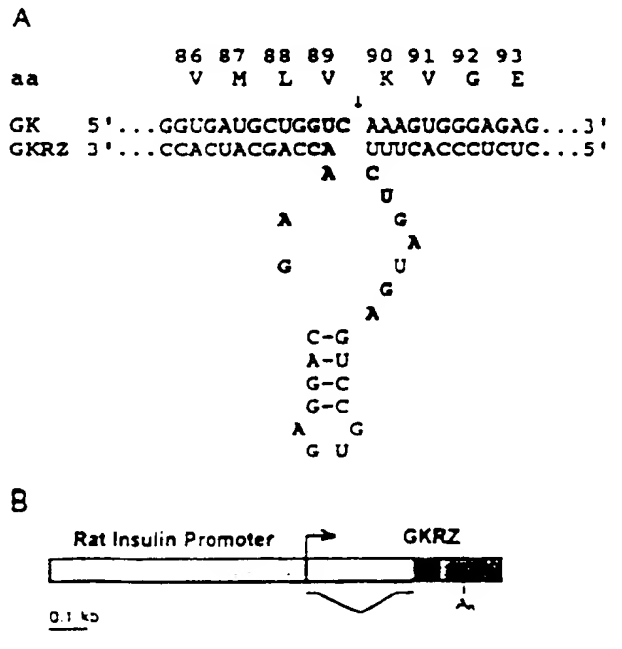

FIG. 1. Design of the RIP-GKRZ construct. (*A*) GKRZ transcript hybridized with the target GK mRNA. The conserved ribozyme nucleotides are shown in boldface letters. The arrow marks the putative cleavage site. (*B*) RIP-GKRZ hybrid gene. The gene consists of a synthetic DNA fragment encoding the ribozyme flanked by GK antisense sequences (GKRZ), an upstream intron element, and a downstream polyadenylylation site.

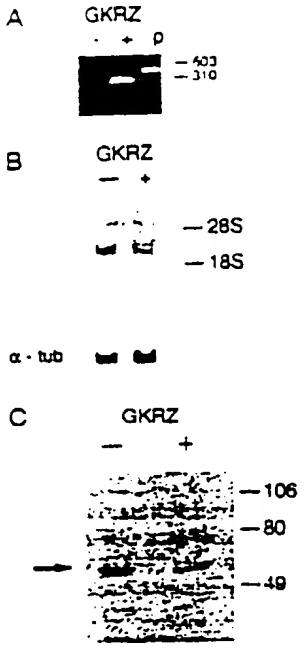

FIG. 2. Analysis of pRIP-GKRZ effect on GK expression in transfected βTC cells. (*A*) Reverse transcriptase–PCR analysis of GKRZ expression in the transfected cells. Expression is manifested by the 200-bp band that results from spliced transcripts. Lane p contains an unspliced fragment amplified from pRIP-GKRZ DNA. Size markers are in bp. (*B*) Northern blotting analysis of GK mRNA. Ribosomal RNA bands serve as size markers. Rehybridization with an α-tubulin probe is shown at the bottom. (*C*) Immunoblotting analysis of GK protein. Size markers are in kDa.

samples in separate lanes were stained with Coomassie blue, and the dried gel was quantitated by densitometry to normalize for protein loading.

Immunohistochemistry. Pancreas samples were sectioned and analyzed with a sheep anti-GK serum as described (19).

Glucose Phosphorylation. Islets were isolated from the pancreas by collagenase infusion through the bile duct (20). Islet homogenates from 1- to 3-month-old mice were incubated with glucose at various concentrations in the presence of ATP, glucose-6-phosphate dehydrogenase, and NAD, and the formation of NADH was monitored fluorimetrically as described (5).

Pancreas Perfusion. Anesthetized 4- to 7-month-old mice were cannulated through the aorta and portal vein and perfused with oxygenated Krebs–Ringer buffer containing glucose in an increasing concentration gradient. Samples were collected and assayed for glucose by a glucose analyzer and for insulin by RIA.

RESULTS

A synthetic DNA fragment was generated that consisted of two 12-bp fragments of mouse GK gene exon 3 sequence (12) in antisense orientation that flank a ribozyme catalytic domain (10, 11) (Fig. 1*A*). This region of the gene was chosen as target because it encodes the putative ATP-binding site of the protein (21). The ribozyme element was introduced to increase the efficiency of the antisense RNA molecules by providing them with the ability to cleave the target mRNA. The hybrid DNA fragment was placed downstream of the rat insulin II promoter and an intron element, and upstream of the simian virus 40 late polyadenylylation site (Fig. 1*B*). Stable transfection of this construct, denoted RIP-GKRZ, into βTC cells resulted in a 45% reduction in GK mRNA

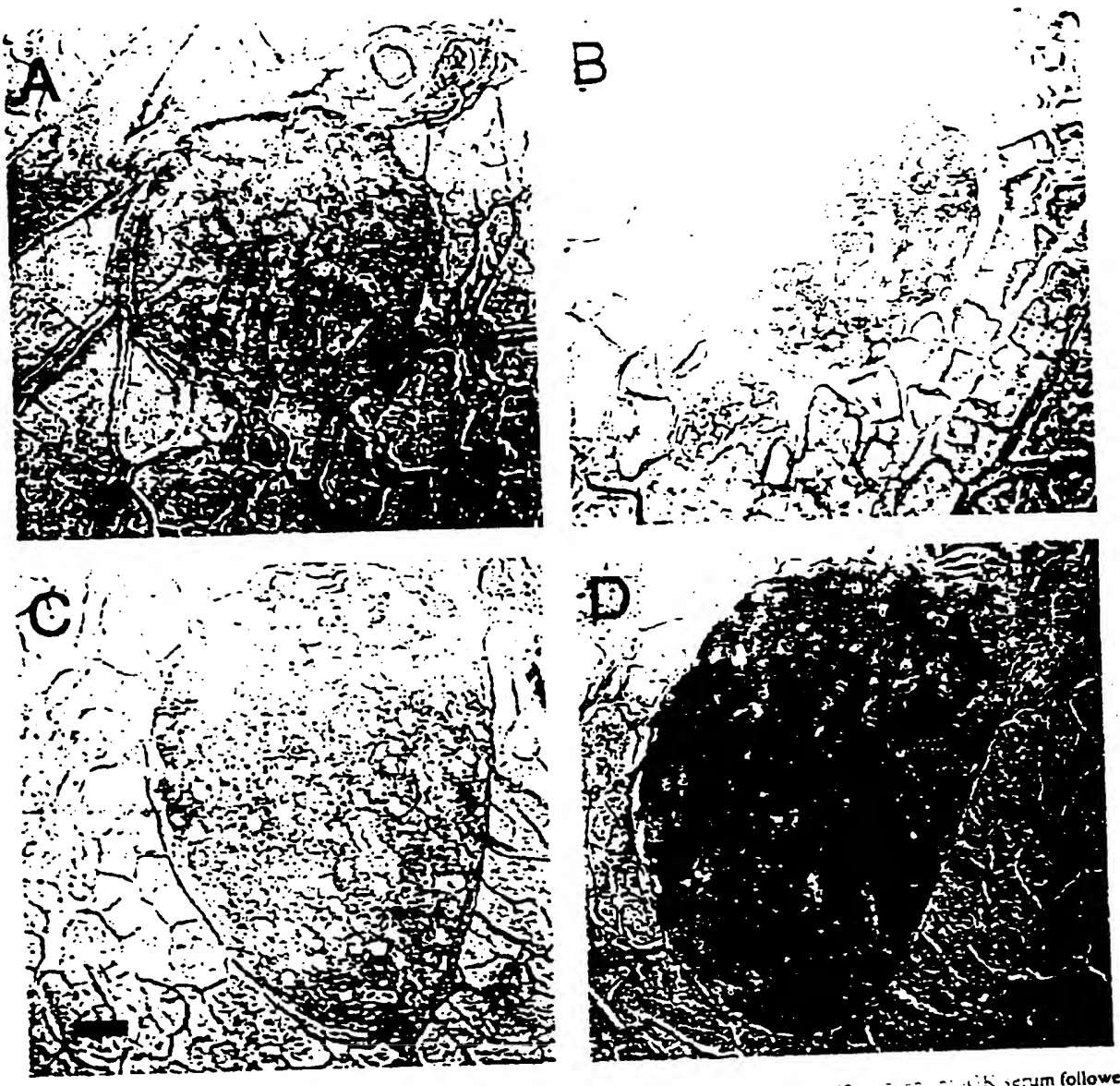

FIG. 3. Immunonistochemical analysis of RIP-GKRZ pancreas. Tissue sections [illegible] GK serum followed by a biotinylated second antibody and were visualized with horseradish peroxidase [illegible] stained with preimmune sheep serum. (*B*) Transgenic islet stained with anti-GK serum. (*C*) Normal [illegible] Normal islet stained with anti-GK serum. (Bar represents 20 μm.)

levels; however, no cleavage products could be detected (Fig. 2*B*). Immunoblotting analysis revealed a 2- to 3-fold reduction in GK protein levels, compared with untransfected cells (Fig. 2*C*). GK activity was reduced from 1.80 ± 0.26 units (U)/g of protein in untransfected cells to 1.07 ± 0.07 U/g (1 U = 1 μmol of product per min). This reduction affected glucose-induced insulin release in these cells only marginally (data not shown), presumably because they contain much higher activities of the low-K_m hexokinases (about 5 U/g of protein) (22), unlike normal islets, in which the predominant activity is that of GK (see Fig. 4).

The RIP-GKRZ construct was microinjected into mouse embryos, and 7 transgenic mouse lineages were generated. Lineages 2 and 4 expressed the transgene, as judged by PCR analysis of islet cDNA. Immunoblotting analysis of isolated islets revealed a 2-fold reduction in islet GK protein, compared with normal islets (data not shown), an effect commensurate to that observed in the transfected cells. Immunohistochemical analysis of pancreas sections with a GK

[illegible] intensity in transgenic [illegible] Fig. 3).

[illegible] amous glucose con- [illegible] method in islets [illegible] in RIP-GKRZ [illegible] normal islets, while [illegible] kinases remained [illegible] in a decrease in [illegible] 5 to 1.3.

[illegible] available from [illegible] type GK allele [illegible] erefore islet GK [illegible] as low or lower [illegible] the RIP-GKRZ [illegible] ose levels (124 ± [illegible] rance (data not [illegible] = 0.12 ng/ml) [illegible] = 0.22 ng/ml). [illegible]old. In contrast,

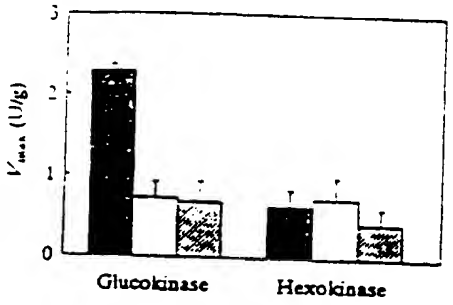

FIG. 4. Glucose phosphorylation activity in RIP-GKRZ islets. V_{max} values of GK and hexokinase were calculated from Eadie–Hofstee plots. The great difference in K_m, 0.05 and 8 mM for hexokinase and GK, respectively, allows us to distinguish the two enzymatic activities. Shaded bar, normal islets; stippled bar, RIP-GKRZ2 islets; hatched bar, RIP-GKRZ4 islets. Values are expressed in U/g of islet protein, as mean ± SEM (n = 3). Transgenic and normal GK activity differences are statistically significant ($P < 0.0001$ by t test).

analysis of glucose-induced insulin secretion from *in situ*-perfused pancreas (Fig. 5) revealed a markedly reduced response of the transgenic pancreas, compared with that of normal controls, in the glucose concentration range of 75–200 mg/dl.

DISCUSSION

These results demonstrate the ability of a hybrid antisense-ribozyme RNA to effect cell-specific changes in gene expression *in vivo*. Expression of the RIP-GKRZ gene resulted in a significant reduction of approximately 70% in both GK protein level and activity. The sequence specificity of this approach is demonstrated by a lack of effect on expression of the related hexokinase genes. Quantitation of GK mRNA in transfected β cells suggests that the attenuation of expression may occur in part through degradation of the target GK transcript. Additional attenuation may be exerted through reduced translational activity of the GK mRNA, presumably by the formation of double-stranded RNA hybrids with the GKRZ transcripts, as has been observed in other antisense RNA experiments (23). Translation of GK mRNA may be particularly sensitive to inhibition in β cells, since GK expression in these cells is regulated mainly at translational and post-translational levels (3, 5). The incomplete inhibition of expression obtained with the antisense approach may represent an advantage for studying its consequences *in vivo*, since it mimics the situation in MODY. In addition, total shut-off of expression may be lethal.

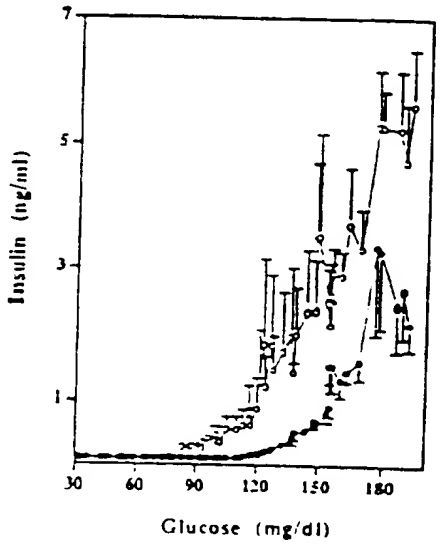

FIG. 5. Insulin secretion from *in situ*-perfused control (○) and transgenic (●) mouse pancreas. Values are mean ± SEM (n = 5).

In spite of the considerable reduction in β-cell GK activity, below the level that gives rise to diabetes in MODY patients, the RIP-GKRZ mice had normal blood glucose and insulin levels. As demonstrated by the perfusion results (Fig. 5), the insulin secretory response to glucose alone is greatly reduced in the transgenic mice, compared with normal controls, in a manner similar to that observed in MODY patients (24). It is possible that in the mouse other insulin secretagogues can compensate for the reduction in glucose-induced secretion. Alternatively, these results may indicate that an impaired liver function, in addition to that of β cells, is required for the induction of overt diabetes by GK deficiency. Such liver impairments have been documented in MODY patients (25). The finding that partial attenuation of expression of the normal GK protein is sufficient to impair the sensitivity of β cells to glucose supports the interpretation of the dominance of the GK mutations in MODY as a gene-dosage effect, rather than a gain-of-function negative dominant effect of the mutant protein.

The reduced β-cell GK activity in the RIP-GKRZ mice may represent a predisposition to diabetes. This may develop into overt disease in certain physiological conditions, such as those caused by age, sex, weight, diet, and genetic background differences. Thus, these mice provide an experimental system for studying the effect of such factors on the development of type II diabetes.

S.E. is supported by the Juvenile Diabetes Foundation International. G.W., Y.-J.W., and M.A.M. are supported by the National Institutes of Health. The oligonucleotide facility of the Albert Einstein College of Medicine is supported by National Institutes of Health Cancer Center Grant.

1. Meglasson, M. D. & Matschinsky, F. M. (1984) *Am. J. Physiol.* 246, E1–E13.
2. Meglasson, M. D. & Matschinsky, F. M. (1986) *Diabetes Metab. Rev.* 2, 163–214.
3. Iynedjian, P. B., Pilot, P. R., Nouspikel, T., Milburn, J. L., Quaade, C., Hughes, S., Ucla, C. & Newgard, C. B. (1989) *Proc. Natl. Acad. Sci. USA* 86, 7838–7842.
4. Magnuson, M. A. & Shelton, K. D. (1989) *J. Biol. Chem.* 264, 15936–15942.
5. Liang, Y., Najafi, H. & Matschinsky, F. M. (1990) *J. Biol. Chem.* 265, 16863–16866.
6. Vionnet, N., Stoffel, M., Takeda, J., Yasuda, K., Bell, G. I., Zouali, H., Lesage, S., Velho, G., Iris, F., Passa, P., Froguel, P. & Cohen, D. (1992) *Nature (London)* 356, 721–722.
7. Stoffel, M., Froguel, P., Takeda, J., Zouali, H., Vionnet, N., Nishi, S., Weber, I. T., Harrison, R. W., Pilkis, S. J., Lesage, S., Vaxillaire, M., Velho, G., Sun, F., Iris, F., Passa, P., Cohen, D. & Bell, G. I. (1992) *Proc. Natl. Acad. Sci. USA* 89, 7698–7702.
8. Gidh-Jain, M., Takeda, J., Xu, L. Z., Lange, A. J., Vionnet, N., Stoffel, M., Froguel, P., Velho, G., Sun, F., Cohen, D., Patel, P., Lo, Y.-M. D., Hattersley, A. T., Luthman, H., Wedell, A., St. Charles, R., Harrison, R. W., Weber, I. T., Bell, G. I. & Pilkis, S. J. (1993) *Proc. Natl. Acad. Sci. USA* 90, 1932–1936.
9. Takeda, J., Gidh-Jain, M., Xu, L. Z., Froguel, P., Velho, G., Vaxillaire, M., Cohen, D., Shimada, F., Makino, H., Nishi, S., Stoffel, M., Vionnet, N., St. Charles, R., Harrison, R. W., Weber, I. T., Bell, G. I. & Pilkis, S. J. (1993) *J. Biol. Chem.* 268, 15200–15204.
10. Forster, A. C. & Symons, R. H. (1987) *Cell* 49, 211–220.
11. Haselloff, J. & Gerlach, W. L. (1988) *Nature (London)* 334, 585–591.
12. Hughes, S. D., Quaade, C., Milburn, J. L., Cassidy, L. & Newgard, C. B. (1991) *J. Biol. Chem.* 266, 4521–4530.

13. Huang, M. T. F. & Gorman, C. M. (1990) *Nucleic Acids Res.* **18**, 937–947.
14. Hanahan, D. (1985) *Nature (London)* **315**, 115–122.
15. Adra, C. N., Boer, P. H. & McBurney, M. W. (1987) *Gene* **60**, 65–74.
16. Hogan, B., Costantini, F. & Lacy, E. (1986) *Manipulating the Mouse Embryo* (Cold Spring Harbor Lab. Press, Plainview, NY).
17. D'Ambra, R., Surana, M., Efrat, S., Starr, R. G. & Fleischer, N. (1990) *Endocrinology* **126**, 2815–2822.
18. Tal, M., Thorens, B., Surana, M., Fleischer, N., Lodish, H. F., Hanahan, D. & Efrat, S. (1992) *Mol. Cell. Biol.* **12**, 422–432.
19. Jetton, T. L. & Magnuson, M. A. (1992) *Proc. Natl. Acad. Sci. USA* **89**, 2619–2623.
20. Gotoh, M., Maki, T., Kiyoizumi, T., Satomi, S. & Monaco, A. P. (1985) *Transplantation* **40**, 437–441.
21. Andreone, T. L., Printz, R. L., Pilkis, S. J., Magnuson, M. A. & Granner, D. K. (1989) *J. Biol. Chem.* **264**, 363–369.
22. Efrat, S., Leiser, M., Surana, M., Tal, M., Fusco-DeMane, D. & Fleischer, N. (1993) *Diabetes* **42**, 901–907.
23. Strickland, S., Huarte, J., Belin, D., Vassalli, A., Rickles, R. J. & Vassalli, J.-D. (1988) *Science* **241**, 680–684.
24. Byrne, M., Sturis, J., Clement, K., Vionnet, N., Stoffel, M., Vehlo, G., Froguel, P. & Polonsky, K. (1993) *Diabetes* **42**, Suppl. 1, 131 (abstr.).
25. Sakura, H., Kawamori, R., Kubota, M., Morishima, T., Kamada, T., Akanuma, Y., Yazaki, Y. & Kadowaki, T. (1993) *Lancet* **341**, 1532–1533.

2242–2248 Nucleic Acids Research, 1994, Vol. 22, No. 12

Reduced β2-microglobulin mRNA levels in transgenic mice expressing a designed hammerhead ribozyme

Sten Larsson, Graham Hotchkiss, Michael Andäng, Tommy Nyholm, José Inzunza, Irma Jansson and Lars Ährlund-Richter*
Unit for Molecular Genetics, Center for Biotechnology, Karolinska Institute, Novum, 141 57 Huddinge, Sweden

Received April 5, 1994; Revised and Accepted May 25, 1994

ABSTRACT

We have generated three artificial hammerhead ribozymes, denoted 'Rz-b', 'Rz-c' and 'Rz-d', with different specificities for exon II of the mouse beta-2-microglobulin (β2M) mRNA. In this study we tested for ribozyme mediated reduction of β2M mRNA in a cell line and in transgenic mice. Transfections of either of the Rz-b, Rz-c or Rz-d plasmids into a mouse cell-line (NIH/3T3) revealed reductions of β2M mRNA substrate in each case. Ribozyme expression in individual transfected clones was accompanied with an up to 80% reduction of β2M mRNA levels. Rz-c was selected for a transgenic study. Seven Rz-c transgenic founder animals were identified from which three ribozyme expressing families were established and analysed. Expression of the ribozyme transgene was tested for and detected in lung, kidney and spleen. Expression was accompanied with reduction of the β2M mRNA levels of heterozygous (Rz+/−) animals compared to non-transgenic litter mates. The effect was most pronounced in lung with more than 90% β2M mRNA reduction in individual mice. In summary, expression of our ribozymes in a cell free system, in a cell-line and in transgenic mice were all accompanied with reductions of β2M mRNA levels.

INTRODUCTION

The use of catalytic RNAs, ribozymes, in the study of gene function has attracted great interest during the past years and ribozyme inhibition of gene expression is a rapidly developing field (reviewed in 1 and 2). One ribozyme variant is the so called 'hammerhead' ribozyme (reviewed in 3). The characteristic hammerhead structure is formed by partly well conserved RNA sequences.

'Tailor-made' ribozymes have been successfully used in several studies to target mRNA expression in cell free systems as well as in mammalian cell lines, e.g. HIV-1 mRNAs (4–9), tumour necrosis factor α (10) and c-fos mRNA expression (11). Recently this approach has successfully been used also in transgenic Drosophila (12). To our knowledge, only one report has been published which describes transgenic mice expressing a functional ribozyme (13), though there have been several reports describing transgenic mice expressing anti-sense RNA, which specifically disrupt gene expression (for example 14–18).

Mouse β2M is a 12kD protein which associates with the major histocompatibility complex (MHC) class I proteins such as H-2K, D, L, TL, Qa-1 and Qa-2. Furthermore, it has been demonstrated that β2M associates with other molecules of the immune system i.e. the Fc receptor in neonatal gut cells (19) and the CD1 protein. In addition it induces collagenase activity in fibroblasts (20) and may serve as a chemotactic protein in the foetal thymus (21). Thus, β2M plays an important role for the immune system (reviewed in 22).

MHC class I molecules have also been shown to have several non-immunologic functions, e.g. as differentiation antigens (23, 24), in the functions of hormone receptors (25–29), or even for olfactory cues influencing mating behaviour (30, 31).

Gene targeting via homologous recombination in embryonic stem cells causes a ubiquitous disruption of the targeted gene in all tissues during the whole life span of the animal, including early ontogeny. This approach has previously been successfully used for the β2M gene. From the studies performed by Koller and Smithies −89 (32), and of Zijlistra *et al* −89 (33), it is known that elimination of β2M mRNA and protein expression leads to no major deleterious effects, i.e. mice without β2M protein are viable.

The work presented in this paper is a step towards ribozyme targeting of gene expression in transgenic mice. To achieve this we have generated a 'basal' ribozyme, designed to give optimal flexibility. It allows transcription both *in vitro* from the bacteriophage T7 RNA polymerase promoter and *in vivo* using the enhancer promoter of the cytomegalovirus (CMV) immediate early gene (34). The enhancer/promoter region was inserted into a unique restriction site in the vector, which allows it to be easily exchanged for other enhancer/promoter regions. Also, the ribozyme specificity can readily be altered by exchange of the inserted ribozyme fragment. There are several unique restriction sites left within the vector, which can be used for future cloning of a set of ribozymes with different target sequences as earlier proposed by Chen *et al* −92 (8). In addition, a second ribozyme

*To whom correspondence should be addressed

was included in our construct, which allows self cleavage immediately 3' of the targeting ribozyme generating a specific 3'-end of this ribozyme (35).

Using this basal ribozyme vector we have generated artificial hammerhead ribozymes with different specific target sequences in exon II of the mouse β2M mRNA. They also differ in their length of complementarity.

We have tested our ribozymes in a cell free system, in a cell-line and in transgenic mice. Expression of the ribozymes was accompanied with reduction of β2M mRNA levels.

MATERIALS AND METHODS

Cloning procedures

The immediate early gene enhancer/promoter region from cytomegalovirus (CMV) was inserted into the unique BamHI restriction site in the multiple cloning site of the pBluescript KS (M13⁻) vector (pBSKS, Stratagene). The CMV enhancer/promoter, from the plasmid pSCTGAL-X556, was kindly provided by Dr S.Rusconi.

A sequence was designed to provide a ribozyme with substrate specificity for β2M, as well as for an additional 3' end processing ribozyme (sequence see Fig. 1), which enables self-cleavage of the 5' end of the transcript (35, and below). Two partially complementary oligonucleotides were synthesised (Scandinavian Gene Synthesis AB – SGS, Köping, Sweden) and annealed. Blunt ends were generated, using T4 DNA polymerase or Klenow DNA polymerase, and the resulting DNA fragment was cloned into the unique SmaI site in the pBSKS-CMV plasmid described above, to generate our 'basal' ribozyme vector (Fig. 1).

Rz-b, Rz-c and Rz-d were designed to have different target sites in the β2M mRNA (Fig. 2, for complete β2M sequence see 36). Rz-b has a 15 nt complementarity to the β2M mRNA and the target sequence includes a central GUC motif with the C nt matching genomic sequence position 3129 located within the coding triplet for amino acid 52 of the β2M protein. Rz-c has a 13 nt complementarity (C at nt 3138; aa 55) and Rz-d an 11 nt complementarity (C at nt 3156; aa 61). Complementary oligos containing recognition sequences were synthesised for each new ribozyme (SGS, Köping, Sweden), annealed and exchanged for the MluI/BglII fragment of the 'basal' ribozyme vector (Fig. 1).

DNA sequencing

The ribozyme clones were sequenced by use of the T3 sequencing primer 5'-dATTAACCCTCACTAAAG-3' (Pharmacia LKB Biotechnology). The DNA sequencing reaction was performed as described by Applied Biosystems using the Taq DyeDeoxy™ termination cycle sequencing kit and analysed in an automatic 373A DNA sequencer.

Cell growth and transfections

Monolayer cultures of NIH/3T3 cells were maintained in Dulbeccos modified Eagles medium (DMEM) supplemented with 10% (v/v) foetal calf serum. Sub-confluent cells were transfected with 20 μg of the ribozyme constructions (linearized using ScaI) together with 0.5 μg of a plasmid containing the neomycin resistance gene.The transfection was achieved with calcium phosphate and a 2×HBS solution, pH 6.87 (37, 38). Selection for neomycin resistance was done with G418 (geneticin, Gibco) at the concentration of 400 μg/ml DMEM. Two weeks post-transfection no cell growth could be detected in the control plates (non-transfected plates). In contrast, 3T3 cell colonies were growing in the plates with the transfected cells. Thirty to fifty clones from each transfection were picked and expanded to 10^7 cells for analysis. For the Rz-b, Rz-c and Rz-d transfections, roughly 50% of the clones were shown by Southern blot analysis to carry 1 – 10 copies of the ribozyme DNA (using a KpnI/NcoI fragment from the Rz construct as a probe). Also, as controls, a ribozyme construct in the reverse orientation, relative to the CMV promoter, was cotransfected together with a plasmid containing the neomycin resistance gene. Eighteen out of 28 clones (64%) were found to be positive when tested in Southern blot analysis using the appropriate probes (data not shown).

Generation of transgenic mice

The Rz-c plasmid was linearized with ScaI and microinjected into the male pronuclei of fertilised (CBAxB6)F_1 oocytes. The embryos were re-implanted into pseudo pregnant (CBAxB6)F_1 recipients (39). Three weeks after birth, tail biopsies were taken and genomic DNA was isolated by standard procedures.

DNA and RNA blot analysis

Integration of the transfected DNA constructs was analysed by Southern blot analysis on genomic DNA and mRNA levels were determined by Northern blot analysis on cytoplasmic RNA (NIH/3T3 cells) or total RNA (organs from transgenic mice).

Genomic 3T3 or mouse tail DNA, isolated according to standard procedures, was cleaved with restriction enzyme BamHI and electrophoresed on a 0.7% agarose gel containing 1×TAE.

For RNA preparation the NIH 3T3 cells were lysed in IsoB 0.65% ,Nonidiet-P40 (NP40) followed by fractionation into cytoplasm and nuclei. Cytoplasmic RNA was isolated by phenol extraction (40). Total RNA from mouse organs was isolated by the GITC procedure (41). The RNA content in the samples was determined by spectrophotography. Aliquots of 5 μg of cytoplasmic RNA were electrophoresed in 1% agarose gels containing 1×MOPS and 0.7% formaldehyde.

DNA or RNA was transferred to a GeneScreen™ filter (according to NEN DuPont's protocol). Probe hybridisation was carried out at 65°C overnight, in a buffer containing 0.5M NaP_i (pH 7.2), 7% SDS and 5mM EDTA. After hybridisation the filters were washed at 65 °C 3×5 min and 1×15–60 min in a buffer containing 40 mM NaP_i (pH 7.2) and 1% SDS.

The probe to detect integrated ribozyme DNA was an NcoI/KpnI DNA fragment partly spanning the CMV promoter and the whole ribozyme region (Fig. 1). For BamHI digested genomic DNA this probe detects a 1200 base-pair (bp) fragment and an additional fragment the size of which is dependent on the site of integration. Mouse β2M mRNA was detected by an EcoRI fragment from the mouse β2M cDNA clone D-98S (kindly provided from Dr P Höglund). DNA probes were labelled with [α^{32}P] dCTP using the Megaprime™ DNA labelling system (Amersham RPN 1607).

As an internal standard for RNA loading, the filters were stripped in 50% formamide for 30 minutes at 65°C and reprobed for glyceraldehyde-3-phosphate dehydrogenase (GAPDH). The GAPDH DNA fragment was kindly provided by Dr Anna Berghard. Gels were stained with ethidium bromide for detection of 18S and 28S rRNA to be used as an additional loading standard.

The 'housekeeping' gene used, GAPDH, showed in its self some variation of expression levels in NIH/3T3 cells. From 30 clones, (randomly selected, with normal 3T3 growth behaviour)

3 out of 12 Rz DNA$^+$ (25%) and 5 out of 18 control clones (28%) were omitted due to inconsistent results when the GAPDH signals were compared to the total RNA amount measured using the spectrophotometric and 18S methods. In our evaluations below of the transfected NIH/3T3 cells, only clones for which we found consistent results for the RNA levels when using the spectrophotometric, GAPDH and 18S methods are included. Some variation was observed also for the β2M mRNA levels when control transfected 3T3 clones were compared (e.g. see Fig. 6).

In vitro transcription and substrate cleavage

Standard T7 RNA polymerase *in vitro* transcription was performed following the purchaser's (Promega) protocol including [α^{32}P] UTP. The ribozyme DNA constructs were linearized using the PstI restriction site in the vector. The transcription products were separated on a denaturing 8% Sanger polyacrylamide gel (19aa : 1 bis aa) containing 8M urea.

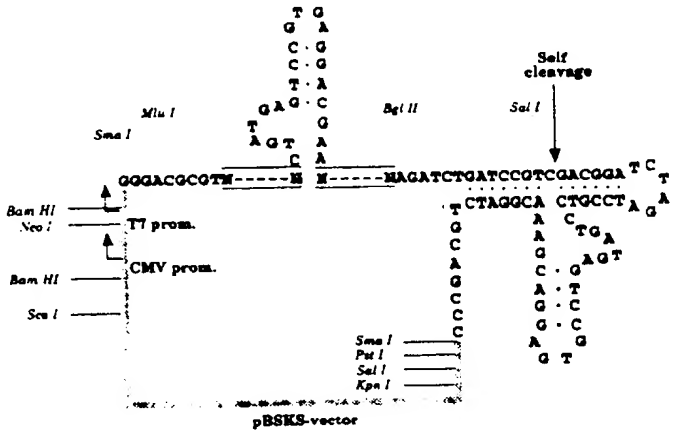

Figure 1. Map of the basal Rz construct showing the projected folding when transcribed. Sequence for the oligonucleotide used to generate the basal ribozyme vector 'Rz' cloned into the SmaI site of the modified M13$^-$ vector pBSKS (Stratagene) is presented. The CMV and T7 promoters are indicated, as well as restriction sites for convenient substitutions of different parts of the ribozyme vector. Boxed areas represent the targetting sequences, that confer substrate specificity to the varient constructs.

The substrate RNA (5'GAUAUGUCCUUCAG-3'; SGS, Köping, Sweden) was 3' labelled with [^{32}P] pCp by ligation using T4 RNA ligase (42). The substrate and a ribozyme transcript were mixed in a buffer containing 20 mM $MgCl_2$ and 50 mM Tris pH 8.0, heated to 95°C for 3 minutes and incubated at 37°C for 30 minutes in a total volume of 15 μl. The reaction was stopped by adding 10 μl of RNA dye and 5 μl of the mixture was separated on a 20% Maxam polyacrylamide gel (29aa : 1 bis aa) containing 8 M urea.

RT-PCR

The Reverse Transcription-Polymerase Chain Reaction (RT-PCR) was performed as described in the protocol from the supplier (GeneAmp® RNA PCR kit, Perkin Elmer Cetus). In short, 3 μl (1 μg) of DNase treated cytoplasmic RNA and 1 μl of a 15 μM 'downstream' primer (5'-TCGTCCTCACGGACTCATC-3'; SGS Köping Sweden), which anneals to the loop in the ribozyme, was mixed with the RT components in the kit. The RT reaction was performed at 42°C for 30 min. For the PCR reaction 1μl of 15μM 'upstream' T7 primer (5'-TAATACGACTCACTATA-GGG-3') and 10μCi (1 μl) [α^{32}P] dCTP per reaction was added to the PCR components. The PCR reaction was performed with 35 cycles, heat denaturation was at 95°C for 1 min, the annealing was at 52°C for 30 sec and the extension time was 45 sec at 60°C. After phenol extraction and ethanol precipitation, the PCR products were separated on a 8% Sanger polyacrylamid gel (19aa: 1 bis aa) containing 8M urea.

RESULTS

Intra-molecular 3' end processing of Rz-b, Rz-c and Rz-d

As a first functional analysis we tested the ability for intra-molecular self-cleavage via the 3'-ribozyme sequence (Fig. 1). The vector was linearized using the PstI site and an *in vitro* T7 RNA polymerase transcription was performed. Figure 3A illustrates a representative transcription of the three ribozymes Rz-b, Rz-c and Rz-d. The result shows that the expected full-length transcripts were produced. In addition, the 3'-end processing ribozyme was, already during the transcription, able to perform the expected self-cleavage reaction (the transcription buffer contains Mg^{2+}), generating the expected β2M-specific ribozyme and the 3'-end ribozyme.

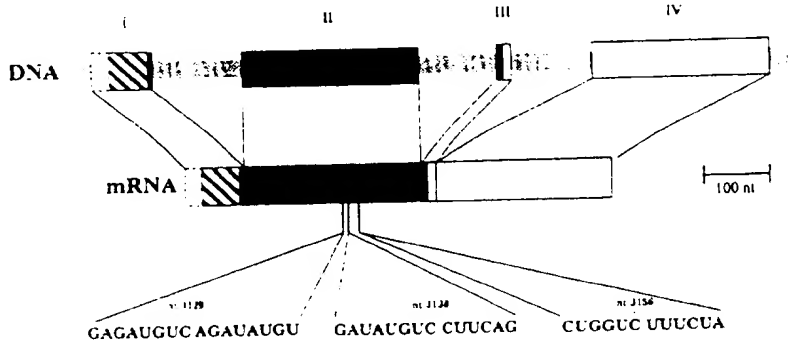

Figure 2. Features of the β2M DNA and mRNA. Open boxes represent untranslated regions, the shaded box represents sequence encoding the signal peptide and filled boxes code for amino acids present in the processed protein (36). Two predominant mRNA species have been described, supposedly differing at their 3' untranslated regions (46). Target sequences for the Rz-b, Rz-c and Rz-d ribozymes and their respective cleavage sites are shown.

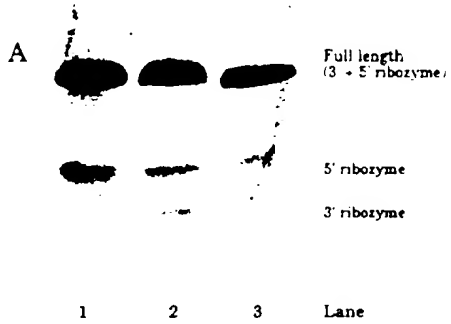

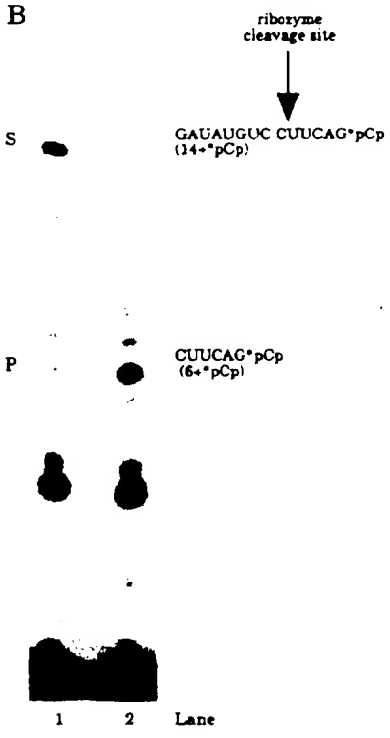

Figure 3. A. *In vitro* transcription of Rz-b, Rz-c and Rz-d using T7-RNA polymerase. The resulting transcripts were separated on an 8% polyacrylamide gel containing 8M urea. The full-length transcripts as well as the β2M specific (5') and 3'-end ribozyme fragments produced by self cleavage are indicated. B. *In vitro* cleavage, by Rz-c, of a short (14 nt + 3' [^{32}P] pCp label) RNA oligonucleotide identical to the 14 nt specific target sequence detected by Rz-c in β2M mRNA (see Fig. 2). Lane 1: substrate; lane 2: substrate + Rz-c. The conditions of the reactions are described in Materials and Methods. Ratio of Rz-c to substrate was approximately 1:1 and the reaction time 30 minutes. The expected fragments produced by cleavage were one 8-mer and one 7-mer. Since the substrate was 3' end labelled, only the 7-mer is visualized. The nt ladder seen is an artefact from the substrate oligo synthesis. We have chosen to show this ladder as a size indicator. Identical results were obtained with gel-purified substrate (not shown). S: substrate, P: product.

Inter-molecular cleavage by Rz-c of its specific substrate

Next, we tested the ability of Rz-c to cleave its specific substrate *in vitro*. Mere incubation of the 15mer (14mer + [^{32}P] pCp) substrate RNA gave no degradation but when the 15mer was mixed with Rz-c a specific cleavage of the substrate took place, generating the expected seven nt long band (6 nt + [^{32}P] pCp): Figure 3B. The reciprocal result was obtained when the RNA was labelled at the 5' end (data not shown).

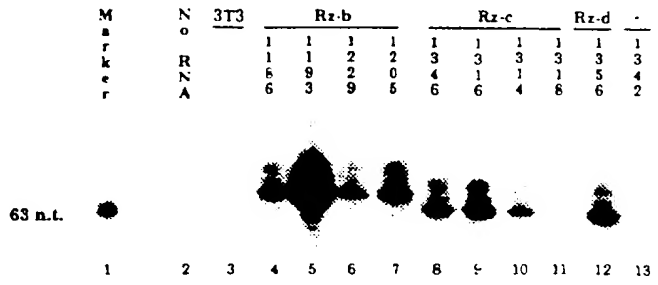

Figure 4. RT-PCR analysis of 3T3 and stable transfectants. Lane 1: size marker; lane 2: RT-PCR components only; lane 3: NIH/3T3 (untransfected cell line), lanes 4–7: clones '1186', '1193', '1229' and '1205' (transfected with and carrying Rz-b + neo), lanes 8–11: clones '1346', '1316', '1314' and '1318' (transfected with and carrying Rz-c + neo), lane 12: clone '1356' (transfected with and carrying Rz-d + neo); lane 13: clone 1342 (transfected with Rz-c – neo, but only carrying neo). RT-PCR using the two specific primers (see Materials and Methods) gives expected fragments of 69 nt (Rz-b) and 67 nt (Rz-c and Rz-d).

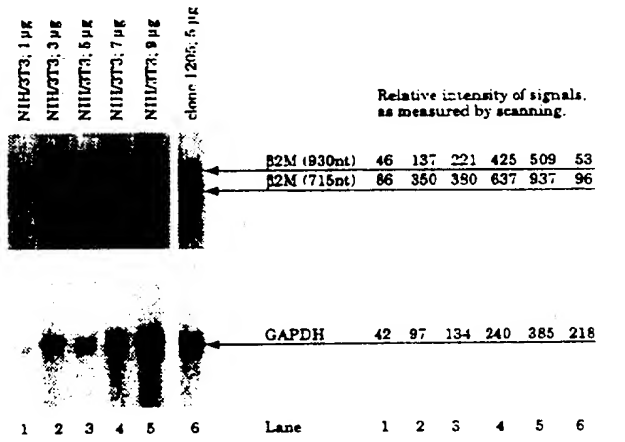

Figure 5. Northern blot analysis of clone 1205 transfected with Rz-b. The β2M expression is correlated to an internal standard, i.e. compared to a 'housekeeping' gene (GAPDH, detected by re-probing), as a control for RNA loading (see text). The GAPDH and β2M signal intensities were measured by scanning with a Shimadzu Chromato-Scanner model Cs-930 (see text) and are indicated above each lane. Lanes 1 - 5: 1,3,5,7 and 9 µg RNA respectively from non-transfected NIH/3T3 cells. Lane 6: 5 µg RNA from clone 1205.

Ribozyme expression in transfected NIH/3T3 clones

Out of nine Rz DNA$^+$ clones (four Rz-b clones: '1186', '1193', '1229', '1205'; four Rz-c clones: '1346', '1316', '1314', '1318' and one Rz-d clone: '1356'), eight expressed the ribozyme (Figure 4, lanes 4–12). The only non-expressing DNA$^+$ clone (clone '1318', lane 11) did not contain the full length insert as judged by Southern blot analysis (data not shown). Clone '1342' (lane 13) was transfected with, but Southern negative for, the Rz-c DNA and subsequently negative for ribozyme expression.

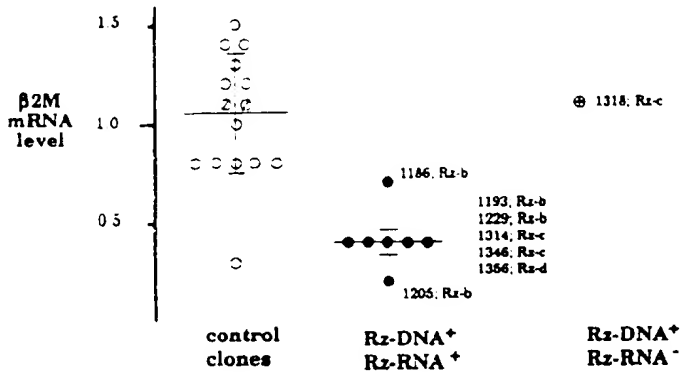

Figure 6. Expression of ribozyme coincides with reduction of β2M mRNA. Each label represents a single clone. The relative β2M mRNA levels were calculated as described in text and Figure 5. All clones were tested in two or three independent Northern blots. Control clones: clones transfected with a construct carrying a reversed orientation Rz (○; n = 13) or transfected with a neomycin resistance gene (Ø; n = 2). Rz-DNA⁻ / Rz-RNA⁻ (●; n = 7) : clones expressing Rz (as indicated and Fig. 4). Rz-DNA⁻ / Rz-RNA⁻ (●; n = 1) : clone '1318' which carries a truncated Rz-DNA, but does not express it (Fig. 4).

β2M mRNA levels in transfected NIH/3T3 cell clones

Figure 5 shows an example of β2M mRNA substrate levels in transfected and non-transfected 3T3 cells. The Northern blot shown is one out of three independent blots of clone '1205' with similar results. Clone '1205' carries approximately five DNA copies of Rz-b (data not shown) and expresses the ribozyme (Fig. 4, lane 7). Based on a spectrophotometric measurement, 5 μg of cytoplasmic RNA from clone 1205, and 1, 3, 5, 7 and 9 μg RNA from non-transfected (control) 3T3 cells, was separated on a 1% agarose gel, transferred to a nylon filter and probed for β2M and GAPDH mRNA (Fig. 5). Scanning of the resulting autoradiograms with a Shimadzu Chromato-Scanner model Cs-930, indicated that the obtained GAPDH signal (from the assumed loaded 5 μg: spectrophotometric measurement) correlated to a GAPDH signal from 5.9 μg of control RNA. (If the obtained GAPDH values are plotted as 'y'-values and the assumed amount of loaded RNA as 'x' values (lanes 1−5), a regression analysis gives an estimated line of $y = 41.5x - 23.6$. Thus, for lane 6 when $y = 218$, this corresponds to $x = 5.9$ μg.) When the signal from the 930 nt β2M mRNA was compared in the same way (5 μg of clone '1205' vs. 1, 3, 5, 7 and 9 μg of control RNA) clone '1205' had a signal intensity as if 1.5 μg of cytoplasmic RNA were loaded . (Plotting of values obtained with the 930 nt band of β2M gives: $y = 99.4x - 19.2$, see above. $y = 53$ corresponds to $x = 1.5$.) The same type of comparison for the 715 nt band gave an apparent load of 1.2 μg. (Plotting of values obtained with the 715 nt band of β2M gives; $y = 60.7x - 35.9$, see above. $y = 96$ corresponds to $x = 1.2$.) From this we conclude that the two species of the β2M mRNA showed a parallel decrease of approximately 75−80%. (1.5 = 25% of 5.9; 1.2 = 20% of 5.9, thus 75−80% reduction.) A similar parallel decrease of the 715 and 930 nt species was found for all other ribozyme expressing clones tested (not shown).

Ribozyme expression coincides with reduced β2M mRNA levels in transfected NIH/3T3 cell clones

Eight Rz DNA⁺/RNA⁻ clones, one Rz DNA⁺/RNA⁻ and fifteen Rz DNA⁻ clones (thirteen containing a ribozyme in the reverse orientation and two only containing the neomycin gene), were studied in detail as described above (Fig. 6).

As expected, the median β2M mRNA value of the control clones, when compared to the 3T3 cell line, was close to 1.0 (arbitrary units). One out of fifteen control clones showed a marked relative reduction of β2M mRNA. The reason for the low β2M mRNA level in this single clone was not analysed further. Clone 1318 (DNA⁺/RNA⁻) showed a β2M mRNA level identical to the median of the control clones and thus no reduction.

In contrast, all clones expressing ribozyme showed reduced β2M mRNA levels compared to the median value of the control clones. The range of the β2M mRNA reduction was between 30−80% with a median of 60%.

Rz-c transgenic mice

One ribozyme construct (Rz-c) was selected for a transgenic study. The ribozyme plasmid was linearised and microinjected into fertilised mouse oocytes. Southern blot analysis identified seven transgenic founder animals. To date three ribozyme expressing families have been established. Offspring from three of these families were analysed on the RNA level in more detail.

Total RNA was isolated from spleen, kidney, and lung. Ribozyme expression was investigated by the RT-PCR assay described above. Figure 7 shows results of the lung from tg+/− individuals from each transgenic family, plus control animals (non-transgenic litter mates). Rz-c was expressed in the lung from the transgene positive animals (lanes 3−5) whereas, as expected, it was not detected in the transgene negative litter mates (Figure 7A, lanes 1−2). Similarly, expression of Rz-c was detected both in spleen and kidney (data not shown).

β2M mRNA levels in Rz-c transgenic mice

Figure 7B shows a northern blot analysis of the same total RNA isolated from lung, hybridised to β2M and GAPDH probes. The results show a reduction of β2M mRNA (for calculations see transfections of NIH/3T3 cells). The expression of the 715 nt β2M mRNA species was reduced by 70% in the family TgN(Rz-c)41Lar, by 22% in TgN(Rz-c)42Lar and 81% in TgN(Rz-c)43Lar. The expression of the 930 nt β2M mRNA species was reduced even more (84%, 58% and 94% respectively).

A more pronounced reduction of the 930 band compared to the 715 band, was consistent also for spleen and kidney (Table 1). This is in contrast to the observation in NIH/3T3 cells where both bands were equally down-regulated (Figure 5). Furthermore, a large variation between individuals within each transgenic family was observed (Table 1).

DISCUSSION

Lacking efficient rules for the designing of reliably potent ribozymes (2), we first decided to use a hammerhead ribozyme using the GUC triplet, conserved in naturally occurring hammerhead ribozymes and proven in *in vitro* studies (43), as the site for substrate cleavage. Furthermore, aided by results in the literature we selected substrate binding sequences with a G/C content of 30−40% and a length of 11−15 nucleotides.

Interestingly, expression of Rz-c as a heterozygous transgene in mice was accompanied with, in some cases, more than 90% reduction of β2M mRNA levels. The variation within a transgenic family was however considerable. The reasons for this variation

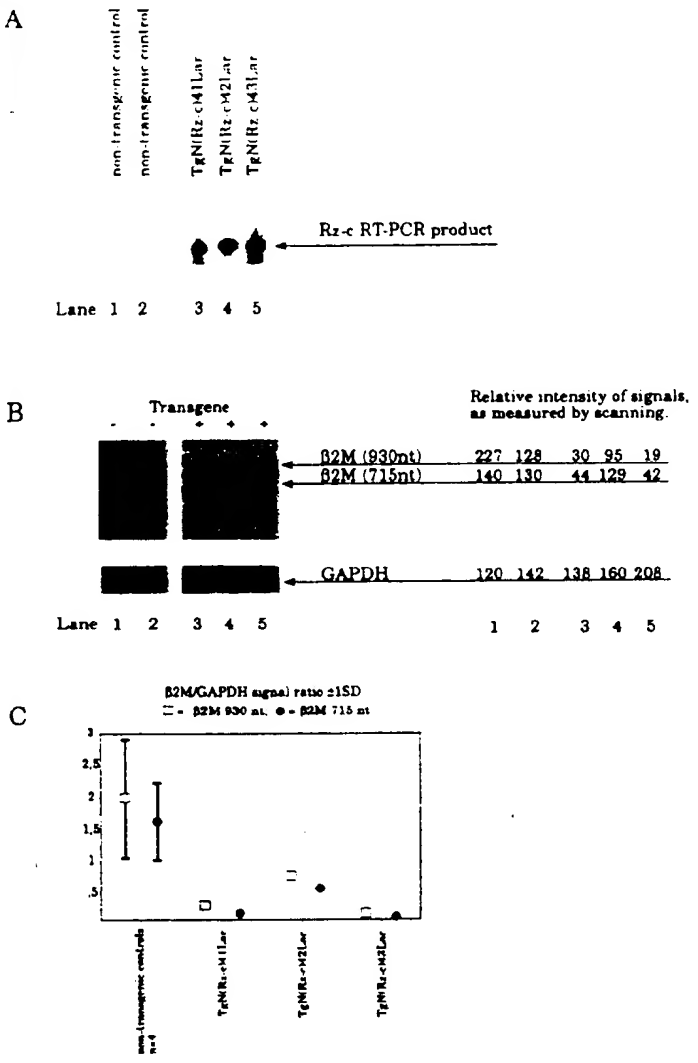

Figure 7. A. RT-PCR analysis of ribozyme expression in Rz-c transgene positive and transgene negative mice. Lanes 1–2: transgene negative control mice (litter mates); lanes 3–5: transgene positive mice. The RT-PCR analysis shows the expected fragment of 67nt representing Rz-c. B. Northern blot analysis of β2M mRNA levels in Rz-c transgene positive and transgene negative mice. The β2M expression (upper part) correlated to an internal standard, i.e. compared to a 'housekeeping' gene (GAPDH, detected by re-probing, lower part) as a control for RNA loading (see text). The GAPDH and β2M signal intensities were measured by scanning with a Shimadzu Chromato-Scanner model Cs-930 (see text) and are indicated in the table next to the Northern blot. Lanes 1–2: transgene negative control mice (litter mates); lanes 3–5: transgene positive mice. C. β2M/GAPDH signal ratio in transgene positive mice (same as in A and B) and non-transgenic littermates.

could be several, but one possibility could be that the CMV promoter/enhancer region used to regulate the Rz-c expression was affected by trans-activating effects from known or unknown viral pathogens in our animal colony. We are currently investigating this intriguing possibility.

Transfections of the ribozyme plasmids into NIH/3T3 cells resulted in reductions of up to 80% of β2M mRNA levels. So ar the analysis does not allow us to determine the relative cleavage efficiency of the three ribozymes, nor to conclusively attribute the concomitant reduction of β2M mRNA to a catalytic effect from the ribozyme.

Table 1. Relative β2M mRNA levels in heterozygous Rz-c transgenic offspring from the TgN(Rz-c)43Lar family, when compared to non-transgenic littermates[1]

	Animal #1 ♀ : 4 months 930 nt / 715 nt	Animal #2 ♀ : 2 months 930 nt / 715 nt	Animal #3 ♂ : 2 months 930 nt 715 nt
Lung	0.1 / 0.20	6 1.0	0.3 / 0.5
Spleen	0.2 / 0.40	9 1.0	0.3 / 0.4
Kidney	0.3 / 1.10	8 0.6	0.1 / 0.1

[1] Calculated as described in text and Figures 5, 6 and 7B. The values are normalized to non-transgenic littermates, the error variation amongst which is shown in Figure 7.

Notably, we used an RT-PCR to detect expression of the ribozymes. Extensive attempts using Northern blot analysis, RNase protection and S1 nuclease assays failed to confidently verify ribozyme expression because of numerous background bands on the autoradiograms (data not shown). We believe this could be due to a high degree of secondary structure (hairpin) in the probes used or, alternatively, to cross reactions with sequences homologous to the hammerhead ribozyme such as U4 and U6 snRNAs (44). We could detect the ribozyme both in the nuclei and in the cytoplasm at an approximate ratio of 1:10 (ribozyme transfected NIH/3T3 cells, data not shown).

Cleavage of a short substrate by Rz-c is in agreement with several other studies (e.g. 1–4, 8, 35). Up to date, few if any report have been presented where a full-length RNA substrate, e.g. mRNA, is cleaved in a cell-free system. We have tried to cleave β2M mRNA both from an *in vitro* transcribed cDNA clone and from isolated cytoplasmic RNA (prepared from NIH/3T3 cells). Both these latter approaches proved unsuccessful, which we believe is due to the high degree of secondary structure in the substrate RNA under the conditions used (data not shown, 45).

A previous report has shown that specific probing of β2M mRNA detects at least two major RNA species, 715 nt and 930 nt (46). In the present study we show that both mRNAs have a similar reduction in ribozyme expressing NIH/3T3 cells. In contrast, we detected an unproportional reduction of the two β2M mRNA species in the transgenic animals. At present we can not explain the discrepancy in these observations. Differences of RNA compartmentalisation (47) between *in vitro* cultured NIH/3T3 cells and the various cell types in the organs tested may account for the results.

Analysis of β2M 'knock-out' mice showed that these healthy mice have a normal distribution of γδ, $CD4^+8^+$ and $CD4^+8^-$ T cells, but no mature $CD4^-8^-$ T cells (32,33). Similarly, we have so far not observed any signs of deleterious effects in the heterozygous Rz-c transgenic mice. Also, since mice heterozygous for the β2M gene disruption have normal β2M protein levels (33) we do not necessarily expect the tg+/− ribozyme mice presented here to be deficient in β2M protein. Breeding to obtain homozygous Rz-c transgenic mice for the analysis of β2M protein levels and presence of mature $CD4^-8^+$ T cells are in progress.

The ribozyme approach offers a potential complement to homologous recombination. Since ribozymes do not affect their target genes at the DNA level, it seems conceivable that the down regulation could be lifted by control of ribozyme expression. The use of carefully chosen transcriptional cassettes e.g. regulatory elements from developmentally regulated genes, or genes

induceable by external stimuli should enable both temporal and spatial control of mRNA targeting in transgenic animals. Thus, the ribozyme method seems to have a potential for applications, directly or indirectly, in functional analysis in cancer research, and also in developmental biology, neurobiology, and molecular biology.

ACKNOWLEDGEMENTS

The authors are grateful to Professor Rolf Ohlsson, the late Professor Håkan Persson and Dr Carlos Ibáñes for valuable discussions, especially during the first feeble steps of this project. This work was supported by grants from The Swedish Cancer Society, Axel och Margaret Ax:son Johnssons Stiftelse, The Swedish Medical Research Council, Lars Hierta Foundation and funds at the Karolinska Institute. G. H. was a recipient of a fellowship from B & K Universal Ltd.

REFERENCES

1. Cech, T. and Bass, B. (1986). *Annu. Rev. Biochem.* 55, 599–629.
2. Rossi, J.J. (1993) *Methods*: A companion to Methods in Enzymology 5, 1–5.
3. Symons, R. H. (1989) *Trends Biochem.* 14, 445–450.
4. Sarver, N., Cantin, E.M., Chang, P.S., Zaia, J.A., Ladne, P.A., Stephens, D.A. and Rossi, J.J. (1990) *Science* 247, 1222–1225.
5. Goodchild, J. and Kohli, V. (1991) *Arch. Biochem. Biophys.* 284, 386–391.
6. Lorentzen, E. U., Wieland, U., Kühn, J. and Braun, R.W. (1991) *Virus Genes* 5, 17–23
7. Weerasinghe, M., Liem, S.E., Asad, S., Read, S.E. and Joshi, S. (1991) *J. Virol.* 65, 5531–5534.
8. Chen, C-J., Banerjea, A.C., Harmison, G.G., Haglund, K., Schubert, M. (1992) *Nucl. Acids Res.* 20, 4581–4589.
9. Heidenreich, O. and Eckstein F. (1992) *J. Biol. Chem.* 267, 1904–1909.
10. Sioud, M., Natvig, J.B. and Forre, O. (1992) *J. Mol. Biol.* 223, 831–835.
11. Scanlon, K. J., Jiao, L., Funato, T., Wang, W., Tone, T., Rossi, J.J. and Kashani-Sabet, M. (1991) *Proc. Natl. Acad. Sci. USA* 88, 10591–10595.
12. Zhao, J.J. and Pick, L. (1993) *Nature* 365, 448–451.
13. Efrat, S., Leiser, M., Wu, Y-J., Fusco-DeMane, D., Emran, O. A., Surana, M., Jetton, T.L., Magnuson, M.A., Weir, G. and Fleishcer, N. (1994) *Proc. Natl. Acad. Sci. USA* 91, 2051–2055.
14. Katsuki, M., Sato, M., Kimura, M., Yokoyama, M., Kobayashi, K. and Nomura, T. (1988) *Science* 241, 593–595.
15. Han, L., Yun, J.S. and Wagner, T.E. (1991) *Proc. Natl. Acad. Sci. USA* 88, 4313–4317.
16. Pepin, M-C., Pothier, F. and Barden, N. (1992) *Nature* 355, 725–728.
17. Moxham, C.M., Hod, Y. and Malbon C.C. (1993) *Science* 260, 991–995.
18. Davis, B.M., Lewin, G.R., Mendell, L.M., Jones, M.E. and Albers, K.M. (1993) *Neuroscience* 56, 789–92.
19. Simister, N. E. and Mostov, K. E. (1989) *Nature* 337, 184–187.
20. Brinckerhoff, C. E., Mitchell, T.I., Karmilowicz, M.J. Klue-Beckerman, B. and Benson, M.D. (1989) *Science* 243, 655–657.
21. Dargemont, C., Dunon, D., Deugnier, M.A., Denoyelle, M., Girault, J.M., Lederer, F., Le, K.H., Godeau, F., Thiery, J.P. and Imhof, B.A. (1989) *Science* 246, 803–806.
22. Ljungren, H-G. (1992) *The Cancer Journal* 5, 308–315.
23. Bartlett, P. F. and Edidin, M. (1978) *J. Cell Biol.* 77, 377–388.
24. Curtis, A. S. G. and Rooney, P. (1979) *Nature* 281, 222–223.
25. Schreiber, A. B., Schlessinger, J. and Edidin, M. (1984) *J. Cell. Biol.* 98, 725–731.
26. Kittur, D., Shimizu, Y., De Mars, R. and Edidin, M. (1987) *Proc. Natl. Acad. Sci. USA* 84, 1351–1355.
27. Solano, A. R., Cremaschi, G., Sanches, M.L., Borda, E., Sterin-Borda, L. and Podesta, E.J. (1988) *Proc. Natl. Acad. Sci. USA* 85, 5087–5091.
28. Olsson, L. (1989) *Proc. Natl. Acad. Sci. USA* 86, 3123–3126.
29. Verland, S., Simonsen, M., Gammeltoft, S., Allen, H., Flavell, R.A. and Olsson, L. (1989) *J. Immun.* 143, 945–951.
30. Singh, P. B., Brown, R.E. and Roser, B. (1987) *Nature* 327, 161–164.
31. Yamazaki, K., Beachamp, G.K., Kupniewski, D., Bard, J., Thomas, L. and Boyse, E.A. (1988) *Science* 240, 1331–1332
32. Koller, B. H. and Smithies, O. (1989) *Proc. Natl. Acad. Sci. USA* 86, 8932–8935.
33. Zijlstra, M., Li, E., Sajjadi, F., Subramani, S. and Jaenish, R. (1989) *Nature* 342, 435–438.
34. Rusconi, S., Severne, Y., Georgiev, O., Galli, I. and Wieland, S. (1990) *Gene* 89, 211–221.
35. Taira, K., Oda, M., Shinshi, H., Maeda, H. and Furkawa, K. (1990) *Protein Eng.* 3, 733–737.
36. Parnes, J.R. and Seidman J.G. (1982) *Cell* 29, 661–669.
37. Graham, F. L. and van der Eb, A. J. (1973). *Virology* 52, 456–467.
38. Wigler, M., Pellicer, A., Silverstein, S. and Axel, R. (1978) *Cell* 14, 725–731.
39. Hogan, B. and Constantini, F. (1986) A laboratory manual C. S. H.
40. Brawerman, G., Mendecki, J. and Lee S.Y. (1972) *Biochemistry* 11, 637–641.
41. Maniatis, T. Fritsch, E. F. and Sambrook, J. (1982) Molecular cloning: A laboratory manual C. S. H.
42. Conway, L. and Wickens, M. (1987) *EMBO J.* 20;6 (13), 4177–4184.
43. Haseloff, J. and Gerlach, W.L. (1988) *Nature* 334, 585–591.
44. Yang, J-H., Cedergren, R. and Nadal-Ginard, B. (1994) *Science* 263, 77–81.
45. Van der Vlugt, R.A.A., Prins, M. and Goldbach, R. (1993). *Virus research.* 27,185–200.
46. Parnes, J.R., Robinson, R.R. and Seidman, J.G. (1983) *Nature* 302, 449–452.
47. Sullenger, B.A. and Cech T.R. (1994) *Science* 262, 1566–1569.

Proc. Natl. Acad. Sci. USA
Vol. 93, pp. 754–758, January 1996
Pharmacology

Nuclease-resistant ribozymes decrease stromelysin mRNA levels in rabbit synovium following exogenous delivery to the knee joint

CRAIG M. FLORY*†, PAMELA A. PAVCO‡, THALE C. JARVIS‡, MARK E. LESCH*, FRANCINE E. WINCOTT‡, LEONID BEIGELMAN‡, STEPHEN W. HUNT III*, AND DENIS J. SCHRIER*

*Department of Immunopathology, Parke-Davis Pharmaceutical Research, Division of Warner-Lambert Company, Ann Arbor, MI 48105; and ‡Ribozyme Pharmaceuticals Inc., Boulder, CO 80301

Communicated by Pedro Cuatrecasas, Parke-Davis Pharmaceutical Research, Ann Arbor, MI, September 25, 1995

ABSTRACT **Catalytic RNA molecules, or ribozymes, have generated significant interest as potential therapeutic agents for controlling gene expression. Although ribozymes have been shown to work *in vitro* and in cellular assays, there are no reports that demonstrate the efficacy of synthetic, stabilized ribozymes delivered *in vivo*. We are currently utilizing the rabbit model of interleukin 1-induced arthritis to assess the localization, stability, and efficacy of exogenous antistromelysin hammerhead ribozymes. The matrix metalloproteinase stromelysin is believed to be a key mediator in arthritic diseases. It seems likely therefore that inhibiting stromelysin would be a valid therapeutic approach for arthritis. We found that following intraarticular administration ribozymes were taken up by cells in the synovial lining, were stable in the synovium, and reduced synovial interleukin 1α-induced stromelysin mRNA. This effect was demonstrated with ribozymes containing various chemical modifications that impart nuclease resistance and that recognize several distinct sites on the message. Catalytically inactive ribozymes were ineffective, thus suggesting a cleavage-mediated mechanism of action. These results suggest that ribozymes may be useful in the treatment of arthritic diseases characterized by dysregulation of metalloproteinase expression.**

The discovery that certain RNA species possess autocatalytic activity (1–3) has generated significant interest in the potential therapeutic use of catalytic RNA molecules, or ribozymes, in controlling gene expression (4). Naturally occurring ribozymes come in a variety of structural motifs (5). Although most ribozymes evolved to cleave their target sequences in cis, ribozymes have also been shown to function in trans (6, 7). Thus, ribozymes have exceptionally broad potential as therapeutic agents for the selective control of gene expression. Of the naturally occurring ribozymes, the hammerhead (8) is the smallest of the known ribozyme motifs and therefore the most amenable to chemical synthesis. It is also well characterized with respect to kinetic parameters and optimal target sequence, and potential cleavage sites are abundant on most messages.

To develop therapeutic ribozymes, significant research has been devoted to improving catalytic activity, developing nuclease resistance, and optimizing the intracellular delivery of both synthetic and expressed ribozymes (8–11). Synthetic ribozymes have shown efficacy in cell culture in reducing the expression of tumor necrosis factor-α (12), bcr-abl (13), and MDR-1 (14). These studies utilized either chemically synthesized chimeric ribozymes with DNA binding arms to increase nuclease resistance or *in vitro* transcribed ribozymes that are protected in part from degradation by being complexed with cationic lipids. We have used ribozymes that contain novel modifications that allow significant catalytic activity while substantially enhancing their nuclease resistance (15).

There are only a few examples of ribozyme activity *in vivo*, and these involve expression of the ribozyme as a transgene either in *Drosophila* (16) or in mice (17, 18). Demonstration of *in vivo* efficacy represents an important advance in the development of synthetic ribozymes as therapeutic agents.

The matrix metalloproteinases (MMPs) are a group of enzymes that degrade extracellular matrix components such as the collagens, gelatins, proteoglycans, and fibronectin (19). Although MMPs play an important role in embryogenesis and normal tissue remodeling (20), abnormal expression may contribute to such disease processes as atherosclerosis (21), cancer (22), and arthritis (23). Stromelysin (MMP3) may be a key mediator in arthritic diseases. It degrades proteoglycans and a broad spectrum of other matrix components (19), and it can readily degrade cartilage *in vitro* (24). Stromelysin also has the capacity to activate the proenzyme forms of collagenase (25), and the 72- (26) and 92-kDa (27) gelatinases, thus initiating a proteinase cascade. Unlike normal synovial fibroblasts, those derived from osteoarthritic or rheumatoid synovium produce high levels of stromelysin and collagenase upon stimulation (28). Most relevant, however, is the marked upregulation of stromelysin and other MMPs seen in articular tissues from patients with osteo- or rheumatoid arthritis (29, 30). It seems likely therefore that inhibiting stromelysin would be a valid therapeutic approach for arthritis.

In the rabbit, injection of human recombinant interleukin 1α (IL-1α) into the knee joint leads to leukocyte accumulation in the joint space, loss of proteoglycan from the articular cartilage, and release of proteoglycan fragments into the synovial fluid (31). An increase in the levels of the MMPs stromelysin and collagenase in the rabbit articular tissues also occurs after stimulation with IL-1 (32, 33). These attributes make it an appropriate model for assessing the role of proteases involved in the pathophysiology of joint disease. We are using this model to assess the localization, stability, and efficacy of exogenous antistromelysin hammerhead ribozymes. These ribozymes are modified to enhance their resistance to nucleolytic degradation (34). We found that ribozymes are taken up by cells in the synovial lining after intraarticular administration. The ribozymes demonstrate good stability in the synovium and can significantly reduce the synovial levels of IL-1-induced stromelysin mRNA. Catalytically inactive ribozymes had little effect on stromelysin mRNA levels. This report demonstrates efficacy of an exogenous synthetic ribozyme *in vivo*.

MATERIALS AND METHODS

Ribozyme Synthesis and Sequences. Ribozymes were synthesized and purified as described by Wincott et al. (35). The

The publication costs of this article were defrayed in part by page charge payment. This article must therefore be hereby marked "*advertisement*" in accordance with 18 U.S.C. §1734 solely to indicate this fact.

Abbreviations: MMP, matrix metalloproteinase; IL, interleukin.

†To whom reprint requests should be addressed.

hammerhead ribozyme motif used in this study contains binding arms (7–8 nt), which can anneal to the stromelysin message, and an invariant core sequence (22 nt) required for catalytic activity. Ribozymes designated as inactive contain the same binding arm sequences as their active counterparts but have two mutations in the core that eliminate cleavage activity. Scrambled ribozymes have the catalytically active core, but the arm sequence is scrambled to eliminate binding to the target sequence.

The sequences of the ribozymes used are given below. Ribozymes are named for their position of cleavage in the human stromelysin sequence. In cases in which the rabbit site was not homologous with human, the rabbit-specific ribozyme is indicated with an R. Lowercase indicates 2′-*O*-methyl nucleotides, uppercase indicates 2′-hydroxyl (ribo) nucleotides, T indicates 3′-3′ inverted thymidine (iT), and μ indicates 2′-amino at positions U4 and U7.

Site 1049, active:	5′-gaaggaacμGAμGaggccgaaaggccGaaAgauggcT
Site 1049, inactive:	5′-gaaggaacμuAμGaggccgaaaggccGauAgauggcT
Site 1049, scrambled:	5′-ugaagagcμGAμGaggccgaaaggccGaaAcggaagT
Site 1363, active:	5′-cuucaaacμGAμGaggccgaaaggccGaaAcagcauT
Site 1366R, active:	5′-augcuuccμGAμGaggccgaaaggccGaaAaaacagT
Site 1410, active:	5′-aaacacccμGAμGaggccgaaaggccGaaAcugugaT
Site 883, active:	5′-cuggaggccμGAμGaggccgaaaggccGaaAcagguucT
Site 1489R, active:	5′-ugccuuccμGAμGaggccgaaaggccGaaAuacaccT

Unless otherwise indicated, backbone linkages are phosphodiester. These ribozymes are designated U4, U7 NH2, and 3′-iT. In some cases, the ribozymes contained four phosphorothioate linkages at the 5′ end (designated U4, U7 NH2, 4 5′ P=S, and 3′-iT). An alternative chemistry of ribozyme 1049 was also used in which position U4 was 2′-*C*-allyl, position U7 was 2′-*O*-methyl, and five phosphorothioate linkages were included on both the 5′ and 3′ ends (U4 *C*-allyl, 5&5 P=S). The catalytic cleavage activity of all of the ribozymes was verified on a complementary short substrate by standard methods; inactive ribozymes did not exhibit any detectable cleavage activity under these conditions (data not shown).

***In Vivo* Localization and Stability of Ribozymes Delivered Intraarticularly.** Male New Zealand White rabbits (3–4 kg) were anesthetized with ketamine·HCl/xylazine and injected intraarticularly with ≈15 × 10^6 cpm (corresponding to 30 ng) of ^{32}P internally labeled ribozyme combined with 10 μg of unlabeled ribozyme in a total vol of 0.5 ml of phosphate-buffered saline (PBS). At various times thereafter, animals were euthanized, the knee joints were lavaged, and synovial tissue was removed, weighed, and either snap frozen for sectioning and autoradiography or placed in Trizol reagent (GIBCO/BRL) for RNA extraction. After initial homogenization of the synovial tissues for RNA extraction, an aliquot was removed to estimate cpm per mg of synovial tissue (assuming that 20% of the synovium was harvested). After extraction of total RNA from the synovial tissue, equal amounts of RNA were run on a denaturing 5% acrylamide gel and the gel was exposed to x-ray film for densitometric quantitation.

***In Situ* Hybridization.** *In situ* hybridization studies were carried out using full-length antisense RNA probes generated by *in vitro* transcription of linearized pRC/CMV plasmid (Invitrogen) containing an ≈1500-bp rabbit stromelysin cDNA (gift of C. Brinckerhoff, Dartmouth Medical School). Samples of synovial tissue were removed, snap frozen in liquid nitrogen, and stored at −80°C. Frozen sections (4–6 μm) were placed on poly(L-lysine)-treated slides and stored at −20°C. Modifications of previously described methods were used (36).

Efficacy Studies. Rabbits were anesthetized with ketamine·HCl/xylazine and injected intraarticularly through the suprapatellar ligament of both knees with various amounts of ribozyme in 0.5 ml of PBS or in PBS alone. Twenty-four hours after ribozyme administration, each rabbit received 25 ng of recombinant human IL-1α (Genzyme) in one knee and vehicle (PBS/0.2% fetal bovine serum) in the other. The synovium was harvested 6 hr after IL-1 infusion, snap frozen in liquid nitrogen, and stored at −80°C.

Table 1. Distribution of radioactivity after intraarticular administration of radiolabeled ribozyme

	Time after ribozyme administration	Synovial tissue*	Synovial RNA	Synovial lavage fluid
Exp. 1	4 hr	4.0	0.03	0.17
	24 hr	3.0	0.32	0.01
Exp. 2	24 hr	5.6	0.32	ND
	3 days	3.0	0.33	ND
	7 days	1.2	0.19	ND

^{32}P internally labeled ribozyme (15 × 10^6 cpm; corresponding to 30 ng) was mixed with 10 μg of unlabeled ribozyme before intraarticular injection. Numbers reflect percentage recovery of total administered radioactivity and represent mean values from three separate animals. ND, not determined.

*Assessed by determining radioactivity of an aliquot after the initial homogenization with Trizol.

RNA Analysis. Total RNA was extracted from synovial tissue with Trizol reagent and analyzed by Northern blotting as described (36). After probing with a full-length antisense RNA probe to stromelysin (see above), the blots were stripped and reprobed with a 100-nt complementary RNA probe to 18S rRNA (Ambion, Austin, TX) to normalize for loading and extraction efficiency. After autoradiography, levels of stromelysin and 18S rRNA were quantified on a scanning densitometer and the data were normalized to the 18S values. In some experiments, RNA was analyzed by both Northern blot analysis and RNase protection (P.A.P., unpublished data). The results were essentially the same when assessed by either method.

RESULTS

Delivery of Ribozymes to Rabbit Synovial Tissues. For these studies, ribozyme labeled with ^{32}P at one internal position was administered directly into the intraarticular space. The fate of the labeled ribozyme was assessed 4 and 24 hr postribozyme administration in the first experiment, and 1, 3, and 7 days after administration in the second. The percentage of labeled ribozyme remaining in the synovial tissue remained relatively constant between 4 and 24 hr (Table 1, Exp. 1). In the total RNA fraction, however, there was a 10-fold increase in associated radioactivity during the same time period.[§] Between 1 and 7 days, there was a 2-fold drop in the total RNA radioactivity and a 4-fold drop in synovial radioactivity (Table 1, Exp. 2). Autoradiographic analysis of the synovial tissue at 24 hr demonstrated that the bulk of the radioactivity was associated with the synovial lining and was intracellular (Fig. 1*A*).

The integrity of the labeled ribozyme extracted with the total synovial RNA at the various times is also shown in Fig. 1. At 4 hr no degradation products could be detected, and by 24 hr the ribozyme remained 80–90% intact (Fig. 1*B*). There were no consistent differences in either the amount or the integrity of labeled ribozyme extracted from IL-1-treated and nontreated knees. The substantial increase in labeled ribozyme present at 24 vs. 4 hr noted above was readily apparent. Fig. 1*C* shows ribozyme integrity at 1, 3, and 7 days. Even after

[§]These results may be explained by recent studies which indicate that fluorescent ribozyme present in synovial cells 4 hr after administration is mostly endosomal, while at 24 hr there is a more diffuse cytoplasmic fluorescence (data not shown). Therefore, although the total amount present in the tissues may have been similar at 4 and 24 hr (as assessed by total tissue homogenates), at 4 hr the endosomal ribozymes may have been lost in the RNA extraction if the endosomes were not disrupted during the homogenization procedure.

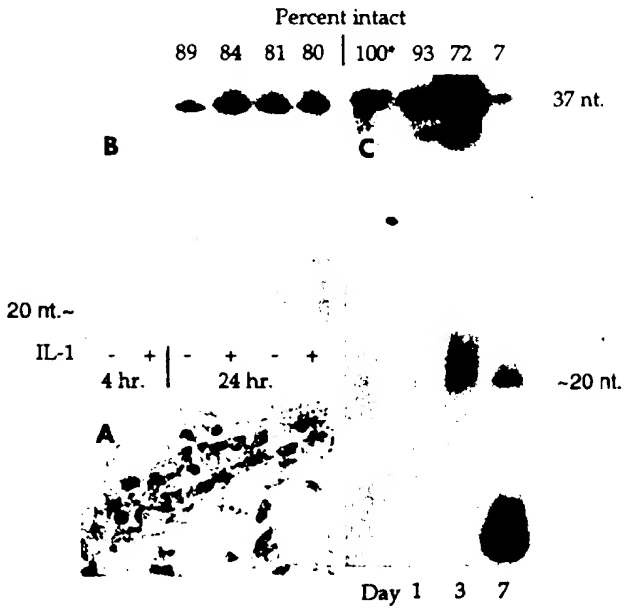

FIG. 1. (*A*) Localization of labeled ribozyme in synoviocytes 24 hr after intraarticular injection. ^{32}P internally labeled ribozyme (15×10^6 cpm; corresponding to 30 ng) was mixed with 10 μg of unlabeled ribozyme before injection. (×340.) (*B*) Stability of labeled ribozyme in synovial tissue 4 and 24 hr after intraarticular administration. Total RNA from synovium (10 μg per lane) was run on a 5% acrylamide/urea gel to assess integrity of the labeled ribozyme. (*C*) Stability of labeled ribozyme in synovial tissue 1, 3, and 7 days after intraarticular administration. The ~20-nt fragment noted in Fig. 2 is the predicted result of endonucleolytic cleavage at two of the unmodified ribonucleotides in the core. *, Sample of ribozyme prior to injection.

7 days, a small amount of full-length ribozyme was still present in synovial tissue.

Stromelysin Expression in Synovial Tissues of IL-1-Treated Rabbit Knees. The kinetics of stromelysin expression after intraarticular injection of 25 ng of IL-1α was assessed by Northern blot (Fig. 2). IL-1 induced a marked but transient increase in the levels of stromelysin mRNA that peaked 6 hr post-IL-1 infusion and returned to near baseline by 24 hr. Saline alone induced a minor but variable increase in stromelysin expression, which followed the same kinetics (data not shown).

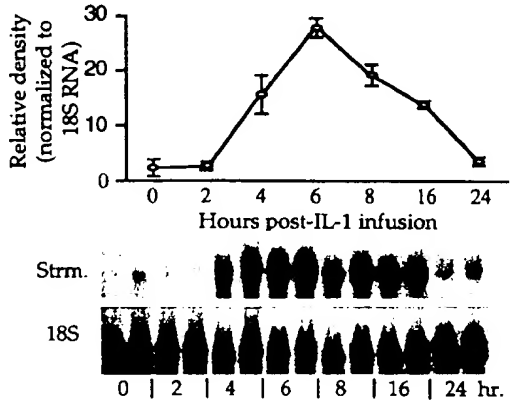

FIG. 2. Kinetics of stromelysin expression after intraarticular injection of 25 ng of IL-1α. Total RNA was extracted from synovial tissue and analyzed by Northern blotting. After probing with a full-length antisense RNA probe to stromelysin, the blots were stripped and reprobed with a 100-nt complementary RNA probe to 18S rRNA to control for equal loading. After autoradiography, stromelysin and 18S rRNA message levels were quantified on a scanning densitometer, and the data were normalized to the 18S values.

FIG. 3. *In situ* hybridization analysis of stromelysin expression in synovial tissue after intraarticular injection of 25 ng of recombinant IL-1α. (*A*) IL-1-stimulated tissues hybridized with antisense complementary RNA probe. (*B*) IL-1-stimulated tissues with sense probe. (*C*) Control tissues from saline-injected knees hybridized with antisense probe. (×100.)

Stromelysin mRNA present in IL-1-induced synovial tissue was also visualized by *in situ* hybridization. Fig. 3*A* illustrates the high level of stromelysin expression observed in the synovial lining from IL-1-treated joints and its absence in the underlying tissue. An adjacent section of IL-1-treated tissue incubated with the sense RNA probe was completely negative (Fig. 3*B*). Fig. 3*C* shows the much reduced expression observed in control, saline-injected knees. Little or no expression was observed in untreated knees (data not shown).

Reduction in Stromelysin mRNA Levels by Intraarticular Delivery of Synthetic Ribozymes. Delivery studies (Fig. 1) demonstrated that peak intact ribozyme levels were observed in the synovium 24 hr after injection. Therefore, we chose to administer ribozyme 24 hr before IL-1 stimulation for the efficacy studies. The synovial tissue was harvested for RNA analysis 6 hr post-IL-1 infusion, the peak of induced stromelysin mRNA levels (Fig. 2).

A representative dose–response curve for ribozyme 1049 (U4, U7 NH2, and 3′-iT) demonstrated a significant reduction in stromelysin message at both the 100 and 300 μg per knee dose of active ribozyme (Fig. 4). At a 1.0-mg dose, the efficacy of the active ribozyme was unchanged or slightly reduced from that seen with the 100-μg dose (data not shown). This ribozyme had been tested on numerous occasions and resulted in an average 60% reduction (ranging from 20% to 80%) in stromelysin message levels compared to the level observed in control, vehicle-treated animals. The inactive ribozyme control retains binding arms identical to the active version but

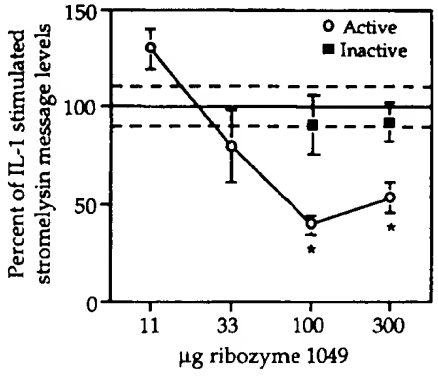

FIG. 4. Dose–response curve of reduction in synovial stromelysin mRNA levels by intraarticular injection of ribozyme 1049, U4, U7 NH2, and 3′-iT. Percentage reduction in IL-1-induced stromelysin message was calculated by using the message level in synovium from saline-injected, non-IL-1-treated joints as the baseline. Data represent two experiments with a total of four animals per dose. Dashed lines represent standard error of IL-1-treated controls. *, Statistically significant difference from IL-1-treated controls ($P < 0.05$).

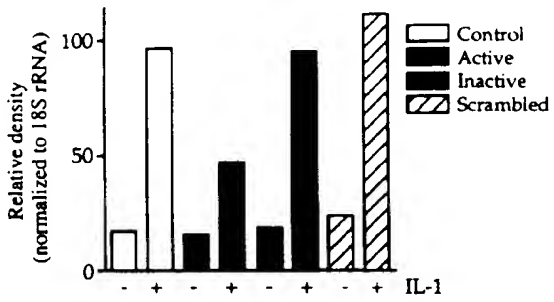

FIG. 5. Reduction in synovial stromelysin mRNA levels by intraarticular injection of ribozyme 1049, U4 *C*-allyl, and 5&5 P=S. Active, inactive, and scrambled ribozymes were tested in parallel. Results from a single animal for each ribozyme are given.

contains a mutated catalytic domain, thus allowing binding to the target sequence but preventing cleavage. There was no significant inhibition of stromelysin mRNA levels by the inactive ribozyme control at any dose.

A number of different chemically modified nucleotides have been developed that confer significant resistance to nucleolytic degradation when incorporated into ribozymes (33). Fig. 5 shows the activity of an alternative stabilized chemical motif targeting the same site, ribozyme 1049. Comparison of Figs. 4 and 5 shows that the two modified ribozymes demonstrate similar efficacy. Fig. 5 also includes a scrambled ribozyme control in which the binding arm sequence of the active ribozyme has been rearranged so that it can no longer bind to its target site on stromelysin mRNA. Like the inactive control, it fails to inhibit stromelysin expression in the synovium. Taken together, these two controls indicate that the ribozyme must bind to and cleave its target site in order to affect the mRNA levels.

The effects of ribozymes that target several different sites in stromelysin message are compiled in Fig. 6. It is clear from these data that not all of the sites tested are equally amenable to ribozyme-mediated cleavage, probably because sites are not equally accessible to ribozyme binding. Ribozymes to sites 1489R and 883 were consistently ineffective, 1410 has shown variable efficacy, and ribozymes to sites 1049, 1366R, and 1363 have shown consistent and relatively equal efficacy. Inactive versions of several of these ribozymes have been tested and have consistently failed to inhibit stromelysin expression (data not shown). A comparison of ribozymes with different 5′ end

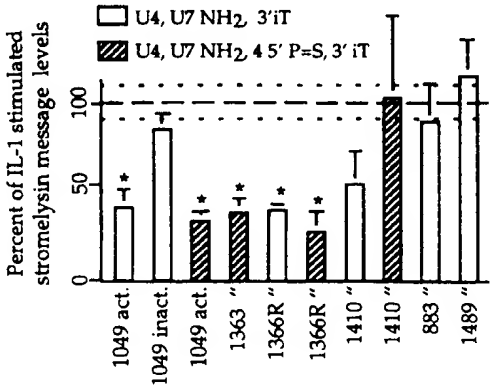

FIG. 6. Reduction in synovial stromelysin mRNA levels by intraarticular injection of ribozymes. Combined data from multiple experiments comparing activity of ribozymes of two different stabilization chemistries and ribozymes directed against different sites on the message. Dotted lines represent standard error of IL-1-treated controls. *, Statistically significant difference from IL-1-treated controls ($P < 0.05$).

modifications (with and without phosphorothioate linkages) is also contained within these data. In general, ribozymes containing phosphorothioate linkages at the 5′ end show similar efficacy compared to non-phosphorothioate-containing ribozymes.

DISCUSSION

We have shown that nuclease-resistant ribozymes injected intraarticularly in rabbits were taken up in the synovial lining and remained ~90% intact at 1 day and 70% intact at 3 days postadministration. Administration of ribozymes directed against stromelysin mRNA resulted in a significant reduction in the levels of IL-1-induced stromelysin message in the synovium. This effect was demonstrated with ribozymes recognizing several distinct sites on the message and with ribozymes of different stabilization chemistries. Although ribozymes to all of the sites were shown to be catalytically active in biochemical assays, several were ineffective *in vivo*. This demonstrates the need for an empirical determination of appropriate target sites. RNA secondary structure or association with cellular proteins may affect target site accessibility. In general, ribozymes that contain mutations that render them inactive were ineffective in reducing stromelysin mRNA levels, thus supporting a cleavage mechanism for ribozyme activity. These results suggest that ribozymes may be useful in the treatment of arthritic diseases characterized by dysregulation of metalloproteinase expression.

Ribozymes have shown potential as a viable approach for the treatment of malignancies and AIDS. In the area of cancer, ribozymes to several different targets have been developed that are capable of reversing the transformed phenotype and reducing cell proliferation or tumorigenicity (13, 37, 38). A variety of ribozymes targeting human immunodeficiency virus have also been reported (39–41). Thus, a body of literature is emerging that illustrates the therapeutic potential for ribozymes in a broad spectrum of disease conditions.

The initial findings that synthetic DNA oligonucleotides (42) or antisense sequences expressed intracellularly (43) could interfere with gene expression have stimulated considerable research in the area of antisense therapeutics. Poor specificity with DNA oligonucleotides has, however, been a recurrent problem with the antisense strategy (44–46). The lack of efficacy observed with inactive ribozyme controls in this study is evidence of a high degree of specificity by ribozymes. In addition, it provides strong support for a cleavage-mediated mechanism of action.

The therapeutic potential of stromelysin ribozymes in the treatment of arthritis remains to be determined. Experiments to evaluate the impact of stromelysin reduction on cartilage proteoglycan levels remain to be done. We do not yet know whether the enzyme levels decrease concordantly with the mRNA or the degree of enzyme reduction necessary to see a therapeutic effect. Because multiple metalloproteinases may be involved in the pathogenesis of arthritis, there may be an advantage in targeting more than one enzyme. In addition, several delivery issues must be addressed. For example, chondrocytes, as well as synoviocytes, produce stromelysin after IL-1 stimulation. We are assessing the relative contribution of these enzyme sources to cartilage proteoglycan loss as well as the ribozyme uptake by these tissues. For chronic conditions such as arthritis, sustained release approaches would be beneficial, and several are under consideration.

1. Kruger, K., Grabowski, P. J., Zaug, A. J., Sands, J., Gottschling, D. E. & Cech, T. R. (1982) *Cell* **31**, 147–157.
2. Zaug, A. J., Grabowski, P. J. & Cech, T. R. (1983) *Nature (London)* **301**, 578–583.
3. Guerrier-Takada, C., Gardiner, K., Marsh, T., Pace, N. & Altman, S. (1983) *Cell* **35**, 849–857.

4. Christoffersen, R. E. & Marr, J. J. (1995) *J. Med. Chem.* **38,** 2023–2037.
5. Castanotto, D., Rossi, J. J. & Deshler, J. O. (1992) *Crit. Rev. Eukaryotic Gene Expression* **2,** 331–357.
6. Zaug, A. J., Been, M. D. & Cech, T. R. (1986) *Nature (London)* **324,** 429–431.
7. Uhlenbeck, O. C. (1987) *Nature (London)* **328,** 596–600.
8. Symons, R. H. (1994) *Curr. Biol.* **4,** 322–330.
9. Cech, T. R. (1992) *Curr. Biol.* **2,** 605–609.
10. Heidenreich, O., Benseler, F., Fahrenholz, A. & Eckstein, F. (1994) *J. Biol. Chem.* **269,** 2131–2138.
11. Yang, J. H., Usman, N., Chartrand, P. & Cedergren, R. J. (1992) *Biochemistry* **31,** 5005–5009.
12. Sioud, M., Natvig, J. B. & Forre, O. (1992) *J. Mol. Biol.* **223,** 831–835.
13. Snyder, D. S., Wu, Y., Wang, J. L., Rossi, J. J., Swiderski, P., Kaplan, B. E. & Forman, S. J. (1993) *Blood* **2,** 600–605.
14. Kiehntopf, M., Brach, M. A., Licht, T., Petschauer, S., Karawajew, L., Kirschning, C. & Herrmann, F. (1994) *EMBO J.* **13,** 4645–4652.
15. Usman, N., Beigelman, L., Draper, K., Gonzalez, C., Jensen, K., Karpeisky, A., Modak, A., Matulic-Adamic, J., DiRenzo, A., Haeberli, P., Tracz, D., Grimm, S., Wincott, F. & McSwiggen, J. (1994) *Nucleic Acids Symp. Ser.* **31,** 163–164.
16. Zhao, J. J. & Pick, L. (1993) *Nature (London)* **365,** 448–451.
17. Larsson, S., Hotchkiss, G., Andang, M., Nyholm, T., Inzunza, J., Jansson, I. & Ahrlund-Richter, L. (1994) *Nucleic Acids Res.* **22,** 2242–2248.
18. Efrat, S., Leiser, M., Wu, Y. J., Fusco-DeMane, D., Emran, O., Surana, M., Jetton, T., Magnuson, M. A., Weir, G. & Fleischer, N. (1994) *Proc. Natl. Acad. Sci. USA* **91,** 2051–2055.
19. Woessner, J. F. (1991) *FASEB J.* **5,** 2145–2154.
20. Werb, Z., Alexander, C. M. & Adler, R. R. (1992) *Matrix Suppl.* **1,** 337–343.
21. Henney, A. M., Wakeley, P. R., Davies, M. J., Foster, K., Hembry, R., Murphy, G. & Humphries, S. (1991) *Proc. Natl. Acad. Sci. USA* **88,** 8154–8158.
22. Stetler-Stevenson, W. G., Aznavoorian, S. & Liotta, L. A. (1993) *Annu. Rev. Cell Biol.* **9,** 541–573.
23. Murphy, G. & Hembry, R. M. (1992) *J. Rheumatol. Suppl.* **32,** 61–64.
24. Bonassar, L. J., Frank, E. H., Murray, J. C., Paguio, C. G., Moore, V. L., Lark, M. W., Sandy, J. D., Wu, J. J., Eyre, D. R. & Grodzinsky, A. J. (1995) *Arthritis Rheum.* **38,** 173–183.
25. Suzuki, K., Enghild, J. J., Morodomi, T., Salvesen, G. & Nagase, H. (1990) *Biochemistry* **29,** 10261–10270.
26. Miyazaki, K., Umenishi, F., Funahashi, K., Koshikawa, N., Yasumitsu, H. & Umeda, M. (1992) *Biochem. Biophys. Res. Commun.* **185,** 852–859.
27. Ogata, Y., Enghild, J. J. & Nagase, H. (1992) *J. Biol. Chem.* **267,** 3581–3584.
28. Brinckerhoff, C. E. & Auble, D. T. (1990) *Ann. N.Y. Acad. Sci.* **580,** 355–374.
29. Hembry, R. M., Bagga, M. R., Reynolds, J. J. & Hamblen, D. L. (1995) *Ann. Rheum. Dis.* **54,** 25–32.
30. Okada, Y., Shinmei, M., Tanaka, O., Naka, K., Kimura, A., Nakanishi, I., Bayliss, M. T., Iwata, K. & Nagase, H. (1992) *Lab. Invest.* **66,** 680–690.
31. Pettipher, E. R., Higgs, G. A. & Henderson, B. (1986) *Proc. Natl. Acad. Sci. USA* **83,** 8749–8753.
32. Mehraban, F., Kuo, S., Riera, H., Chang, C. & Moskowitz, R. W. (1994) *Arthritis Rheum.* **37,** 1189–1197.
33. Hutchinson, N. I., Lark, M. W., MacNaul, K. L., Harper, C., Hoerrner, L. A., McDonnell, J., Donatelli, S., Moore, V. & Bayne, E. K. (1992) *Arthritis Rheum.* **35,** 1227–1233.
34. Beigelman, L., McSwiggen, J., Draper, K., Gonzalez, C., Jensen, K., Karpeisky, A., Modak, A., Matulic-Adamic, J., DiRenzo, A., Haeberli, P., Sweedler, D., Tracz, D., Grimm, S., Wincott, F., Thackaray, V. G. & Usman, N. (1995) *J. Biol. Chem.* **270,** 25702–25708.
35. Wincott, F., DiRenzo, A., Shaffer, C., Grimm, S., Tracz, D., Workman, C., Sweedler, D., Gonzalez, C., Scaringe, S. & Usman, N. (1995) *Nucleic Acids Res.* **23,** 2677–2684.
36. Flory, C. M., Jones, M. L. & Warren, J. S. (1993) *Lab. Invest.* **69,** 396–404.
37. Funato, T., Shitara, T., Tone, T., Jiao, L., Kashani-Sabet, M. & Scanlon, K. J. (1994) *Biochem. Pharmacol.* **48,** 1471–1475.
38. Kobayashi, H., Dorai, T., Holland, J. F. & Ohnuma, T. (1994) *Cancer Res.* **54,** 1271–1275.
39. Yu, M., Poeschla, E., Yamada, O., Degrandis, P., Leavitt, M. C., Heusch, M., Yees, J., Wong-Staal, F. & Hampel, A. (1995) *Virology* **206,** 381–388.
40. Ventura, M., Wang, P., Franck, N. & Saragosti, S. (1994) *Biochem. Biophys. Res. Commun.* **203,** 889–898.
41. Zhou, C., Bahner, I. C., Larson, G. P., Zaia, J. A., Rossi, J. & Kohn, D. B. (1994) *Gene* **149,** 33–39.
42. Zamecnik, P. C. & Stephenson, M. L. (1978) *Proc. Natl. Acad. Sci. USA* **75,** 280–284.
43. Izant, J. G. & Weintraub, H. (1984) *Cell* **36,** 1007–1015.
44. Wagner, R. W. (1994) *Nature (London)* **372,** 333–335.
45. Bennett, C. F., Condon, T. P., Grimm, S., Chan, H. & Chiang, M. (1994) *J. Immunol.* **152,** 3530–3540.
46. Villa, A. E., Guzman, L. A., Poptic, E. J., Labhasetwar, V., D'Souza, S., Farrell, C. L., Plow, E. F., Levy, R. J., DiCorleto, P. E. & Topol, E. J. (1995) *Circ. Res.* **76,** 505–513.